

1  
2  
3  
4  
5  
6  
7  
8  
9  
10  
11  
12  
13  
14  
15  
16  
17  
18  
19  
20  
21  
22  
23  
24  
25  
26

# Revision 1

## MSA PRESIDENTIAL ADDRESS

### Metamorphism and the evolution of subduction on Earth

MICHAEL BROWN<sup>1\*</sup> AND TIM JOHNSON<sup>2</sup>

<sup>1</sup>Laboratory for Crustal Petrology, Department of Geology, University of Maryland, College Park, MD 20742, U.S.A.

<sup>2</sup>School of Earth and Planetary Sciences, The Institute for Geoscience Research (TIGeR), Curtin University, GPO Box U1987, Perth WA 6845, Australia; and, Center for Global Tectonics, State Key Laboratory for Geological Processes and Mineral Resources, China University of Geosciences, Wuhan, Hubei Province, 430074, China

---

\* Email: [mbrown@umd.edu](mailto:mbrown@umd.edu)

#### ABSTRACT

Subduction is a component of plate tectonics, which is widely accepted as having operated in a manner similar to the present-day back through the Phanerozoic Eon. However, whether Earth always had plate tectonics or, if not, when and how a globally-linked network of narrow plate boundaries emerged are matters of ongoing debate. Earth's mantle may have been as much as 200–300 °C warmer in the Mesoarchean compared to the present day, which potentially required an alternative tectonic regime during part or all of the Archean Eon. Here we use a dataset of the pressure ( $P$ ), temperature ( $T$ ) and age of metamorphic rocks from 564 localities that vary in age from the Mesoarchean to the Cenozoic to evaluate the petrogenesis and secular change of metamorphic rocks associated with subduction and collisional orogenesis at convergent plate boundaries. Based on thermobaric ratio ( $T/P$ ), metamorphic rocks are classified into three natural

27 groups: high T/P type ( $T/P > 775^\circ\text{C}/\text{GPa}$ , mean  $T/P \sim 1105^\circ\text{C}/\text{GPa}$ ), intermediate T/P type ( $T/P$   
28 between  $775$  and  $375^\circ\text{C}/\text{GPa}$ , mean  $T/P \sim 575^\circ\text{C}/\text{GPa}$ ), and low T/P type ( $T/P < 375^\circ\text{C}/\text{GPa}$ ,  
29 mean  $T/P \sim 255^\circ\text{C}/\text{GPa}$ ). With reference to published thermal models of active subduction, we  
30 show that low T/P oceanic metamorphic rocks preserving peak pressures  $> 2.5$  GPa equilibrated  
31 at  $P$ - $T$  conditions similar to those modeled for the uppermost oceanic crust in a wide range of  
32 active subduction environments. By contrast, those that have peak pressures  $< 2.2$  GPa may  
33 require exhumation under relatively warm conditions, which may indicate subduction of young  
34 oceanic lithosphere or exhumation during the initial stages of subduction. However, low T/P  
35 oceanic metamorphic rocks with peak pressures of  $2.5$ – $2.2$  GPa were exhumed from depths  
36 where, in models of active subduction, the slab and overriding plate change from being  
37 decoupled (at lower  $P$ ) to coupled (at higher  $P$ ), possibly suggesting a causal relationship. In  
38 relation to secular change, the widespread appearance of low T/P metamorphism in the  
39 Neoproterozoic represents a ‘modern’ style of cold collision and deep slab breakoff, whereas rare  
40 occurrences of low T/P metamorphism in the Paleoproterozoic may reveal atypical localized  
41 regions of cold collision. Low T/P metamorphism is not known from the Archean geological  
42 record, but the absence of blueschists in particular is unlikely to manifest secular change in the  
43 composition of the oceanic crust. In addition, the premise that the formation of lawsonite  
44 requires abnormally low thermal gradients and the postulate that oceanic subduction-related  
45 rocks register significantly lower maximum pressures than do continental subduction-related  
46 rocks, and imply different mechanisms of exhumation, are not supported. The widespread  
47 appearance of intermediate T/P and high T/P metamorphism at the beginning of the Neoproterozoic,  
48 and the subsequent development of a clear bimodality in tectono-thermal environments are

49 interpreted to be evidence of the stabilization of subduction during a transition to a globally-  
50 linked network of narrow plate boundaries and the emergence of plate tectonics.

51

## 52 INTRODUCTION

53 *“Without hypotheses to test and prove or disprove, exploration tends to be*  
54 *haphazard and ill-directed. Even completely incorrect hypotheses may be very*  
55 *useful in directing investigation toward critical details.”* (Hess, 1954, p. 344)

56

57 As the plate tectonics revolution gathered steam during the 1960s, linking sea-floor  
58 spreading with transform faults and subduction, it evolved into a paradigm to describe the  
59 Cenozoic to Mesozoic tectonics of the lithosphere—the strong outer layer of Earth above the  
60 weaker asthenosphere. The theory of plate tectonics developed from geophysical studies of the  
61 ocean basins (Vine and Matthews, 1962; Wilson, 1965; McKenzie and Parker, 1967; Le Pichon,  
62 1968, Morgan, 1968), which extend back in age only to the early Mesozoic, and was confirmed  
63 by seismology (Sykes, 1967; Isacks et al., 1968), which uses contemporary earthquake activity.  
64 The history of the plate tectonics revolution is covered in many books, but for a contemporary  
65 perspective the interested reader is referred to the book by Oreskes *“Plate tectonics: An insider's*  
66 *history of the modern theory of the Earth”* (2002), and for a very readable synthesis of the  
67 development of the theory of plate tectonics to the book by Livermore *“The tectonics plates are*  
68 *moving”* (2018). Plate tectonics has enabled us to understand recent recycling of the lithosphere  
69 and the geodynamics of the contemporary Earth, but has Earth always had plate tectonics?

70 Notwithstanding the absence of pre-Mesozoic ocean basins, plate tectonics is widely  
71 accepted as having operated in a manner similar to the present-day back through the Phanerozoic

72 Eon (e.g., Stern 2005, 2018). By contrast, applying this paradigm to the Precambrian has led to  
73 debate about when and how plate tectonics first emerged on Earth. This uncertainty occurs not  
74 only because plate tectonics destroys oceanic lithosphere—the critical evidence for its operation  
75 during the past 200 Ma—at convergent plate boundaries, leaving only imprints of plate boundary  
76 processes stored in the continents, but also because Earth’s mantle was warmer in the past than at  
77 the present day, although by how much is controversial (Aulbach and Arndt, 2019a,b; Condie et  
78 al., 2016; Herzberg, 2019; Herzberg et al., 2010; Putirka, 2016). A warmer mantle may have  
79 required an alternative tectonic regime during part or all of the Archean Eon.

80         Despite a growing consensus that Earth had adopted plate tectonics by sometime in the  
81 late Archean (Brown, 2006; Sizova et al., 2010, van Hunen and Moyen, 2012; Cawood et al.,  
82 2018; Dhuime et al., 2018; Johnson et al., 2019), there are some who argue for plate tectonics as  
83 early as the Hadean (Hopkins et al., 2008; Harrison and Wielicki, 2016; Kusky et al., 2018), or at  
84 least for subduction at that time (Turner et al., 2014), consistent with the null hypothesis that  
85 plate tectonics was the principal mode of heat loss throughout Earth history (Korenaga, 2013,  
86 2018; Foley, 2018). Conversely, there are others who argue against global modern-style  
87 subduction before the Neoproterozoic (Stern, 2005), requiring an alternative paradigm to plate  
88 tectonics for the Hadean to Mesoproterozoic interval (Stern, 2018). Although this divergence of  
89 views has existed for more than a decade, we have arguably not made much progress towards a  
90 resolution (Hawkesworth and Brown, 2018). One reason this has proven to be a difficult issue to  
91 resolve is that the evolution of mantle potential temperature ( $T_P$ ) can be modelled adequately  
92 (Fig. 1) either in a plate tectonic regime with constant surface heat flow and low present-day  
93 Urey ratio or with a switch in heat-flow scaling at relatively low present-day Urey ratio from  
94 stagnant lid (lower heat flow) to plate tectonics (higher heat flow). A changeover from a stagnant

95 lid regime to plate tectonics at 3 Ga or 2 Ga (Korenaga, 2013, 2017) is consistent with the mantle  
96  $T_p$  data of Herzberg et al. (2010), but a changeover at 1 Ga, as argued by Stern (2018), is not  
97 (Fig. 1).

98         If plate tectonics has not been operative throughout Earth history, what preceded it?  
99         Rather than a plate tectonics or ‘mobile lid’ regime, which is governed by the relative motion of  
100 rigid plates of lithosphere, the early Earth may have been characterized by a ‘stagnant lid’ regime  
101 that consisted of a thick, deformable, more-or-less continuous ‘squishy’ lithosphere (Gerya,  
102 2014; Johnson et al., 2014; Sizova et al., 2015; Rozel et al., 2017). This ‘squishy’ lithosphere  
103 may have experienced intermittent subduction, perhaps spontaneously or possibly driven by  
104 large impacts or mantle plumes, and may have undergone overturns leading to extensive  
105 resurfacing (Arndt and Davaille, 2013; O’Neill et al., 2007, 2017, 2018; Gerya et al., 2015;  
106 Sizova et al., 2015). For a warmer mantle, subducting slabs could have had a greater propensity  
107 to breakoff due to their different buoyancy structure (van Hunen and van den Berg, 2008;  
108 Sobolev and Brown, 2019).

109         The creation of a global network of narrow plate boundaries and its maintenance through  
110 time are critical conditions for a plate tectonic mode of geodynamics on any planet (Bercovici  
111 and Ricard, 2014; Lenardic, 2018). Conversely, localized regions of subduction that were not  
112 part of a network of narrow plate boundaries, such as exist on Venus, are not evidence for plate  
113 tectonics (Kaula and Phillips, 1981; Smrekar et al., 2018). Consequently, to argue that plate  
114 tectonics operated on the early Earth requires evidence of a (close to) global network of  
115 connected plate boundaries. Given the limited rock record available for the early Earth and the  
116 inherent preservation biases involved, it may simply not be possible to determine if early Earth  
117 had plate tectonics (Lenardic, 2018). Furthermore, Earth may have evolved into a plate tectonic

118 regime sometime before sufficient evidence of its existence was retained in the global geological  
119 record. Thus, the geological record is only ever likely to provide a lower limit on the emergence  
120 of plate tectonics on Earth.

121 From a geological perspective, how to determine a minimum age for plate tectonics on  
122 Earth may be broken into several components (Cawood et al., 2018). For instance, when did the  
123 lithosphere first behave as a mosaic of plates—torsionally-rigid lithospheric fragments bounded  
124 by a network of narrow zones of plate divergence and generation, transform displacement or  
125 plate convergence and destruction? Related to this question, how far back in time can we identify  
126 independent horizontal motions between different cratons? These questions have been addressed  
127 recently by Cawood et al. (2018). Here we concentrate on the appearance of a linked network of  
128 relatively narrow plate boundaries, which is related to the secular evolution of subduction and  
129 should be evident from the record of crustal metamorphism.

130 The hallmarks of subduction are commonly considered to be the presence of arc  
131 magmatic rocks and low thermal gradient (low  $T/P$ ) metamorphic rocks, such as blueschists and  
132 low-temperature eclogites (Brown, 2006; Pearce et al., 2008; Stern, 2005). However, the  
133 unambiguous identification of arc magmatism in the Archean rock record based mainly on trace  
134 element discrimination is potentially ambiguous and open to interpretation (e.g., Pearce et al.,  
135 2008; Pearce, 2014; Johnson et al., 2016, 2017; Smithies et al., 2018). Furthermore, with a few  
136 exceptions, low  $T/P$  metamorphic rocks are absent from the rock record before the late Tonian,  
137 and in reality it is a duality of thermobaric types of metamorphic that is the true hallmark of  
138 metamorphism related to convergent plate boundaries (Brown, 2006). We emphasize that it is the  
139 widespread imprint of these hallmarks that might identify the operation of plate tectonics, not  
140 simply isolated occurrences, no matter how certain the interpretation. In this study, our goal is to

141 interrogate the rock record both to identify the oldest evidence of stable subduction of oceanic  
142 lithosphere and to assess secular change in the thermobaric ratios of metamorphism associated  
143 with convergent plate boundaries, focusing on orogenic sutures as they have the highest potential  
144 to preserve evidence of subduction in the rock record.

145

## 146 **PLATE TECTONICS AND METAMORPHISM**

147 In the 1970s the relationship between plate tectonics and metamorphism was addressed  
148 by Oxburgh and Turcotte (1971), Ernst (1971, 1973) and Miyashiro (1972, 1973), which placed  
149 Miyashiro's (1961) concept of paired metamorphic belts in a plate tectonics context. Earth's  
150 plate tectonics regime is characterized by asymmetric (one-sided) subduction of ocean  
151 lithosphere at convergent plate boundaries (Gerya et al., 2008). In this regime, the downgoing  
152 slab depresses isotherms creating a 'cool' metamorphic environment, whereas the breakdown of  
153 hydrous minerals generates fluids and melts that promote magma generation in the overlying  
154 mantle wedge leading to 'warm' conditions in the overriding plate. Plate motions lead to  
155 collisions between arcs, ribbon terranes and continents, sometimes involving ocean plateaus,  
156 preserving evidence of low  $T/P$  metamorphism in the suture, and creating thickened lithosphere  
157 to generate intermediate  $T/P$  metamorphism in the mountain belt and high  $T/P$  metamorphism in  
158 the hinterland or back-arc (Brown and Johnson, 2018; Hyndman, 2018).

159 The first evidence of blueschist facies metamorphism occurs in the Neoproterozoic (late  
160 Tonian; Xia et al., 2019; Yong et al., 2013), and this is commonly taken as one indicator of the  
161 beginning of the modern style of subduction and plate tectonics (Stern, 2005). However, on a  
162 warmer Earth prior to the Neoproterozoic, subduction and plate tectonics might have left a  
163 different imprint in the ancient rock record (e.g., Brown, 2006, 2007, 2014). Based on numerical

164 models, it has been suggested that higher mantle temperatures in the past led to a different style  
165 of collision between continents, protocontinents and arcs, particularly in the late Archean–early  
166 Proterozoic (Chowdhury et al., 2017; Perchuk et al., 2018). Furthermore, weaker slabs could  
167 have led to more frequent breakoff, such that subduction might have been intermittent (van  
168 Hunen and van den Berg, 2008; Sizova et al., 2015), preventing subduction of continental crust  
169 to mantle depths (van Hunen and van den Berg, 2008; Sizova et al., 2014).

170 In reading the rock record, in addition to the effects of higher mantle  $T_P$  and crustal heat  
171 production, the role of preservation, the influence of sampling bias and the reliability of data  
172 gaps are other issues to consider. Because the geological record degrades back through time, we  
173 must also weigh regional (commonly older) versus global (commonly younger) datasets, and  
174 distinguish evidence for the localized initiation of subduction (e.g., Turner et al., 2014; Pearce,  
175 2014) from intermittent or transient subduction (e.g., van Hunen and van den Berg, 2008; Moyen  
176 and van Hunen, 2012; Sizova et al., 2015) from present-day globally continuous subduction  
177 (Livermore, 2018).

178 In this article, we test an alternative to the null hypothesis that plate tectonics has always  
179 been the geodynamic mode on Earth, specifically that the stabilization of subduction and the  
180 emergence of plate tectonics across the globe had occurred by the Proterozoic but probably not  
181 much earlier. The transition is shown by the widespread occurrence of two contrasting types of  
182 metamorphism in the Neoproterozoic rock record, which may be evidence of a global distribution of  
183 dual thermobaric environments that are characteristic of subduction and plate tectonics at the  
184 present day (Brown and Johnson, 2018). This may have been a gradual process as a network of  
185 narrow plate boundaries spread across the globe, but appears to have been completed by the



186 Proterozoic when a distinct bimodality in thermobaric ratios began to appear in the crustal record  
187 of metamorphism.

188

189

## CONTEXT

190 This article is based on content from the 2018 Mineralogical Society of America  
191 Presidential Address by the first author. However, it is important to note that it is the last in a  
192 series of three invited articles with a common backbone—a dataset of age and  $P$ – $T$  conditions for  
193 several hundred localities that we consider to be representative of crustal metamorphism from  
194 the Neoproterozoic to the present day. The dataset also contains information from 11 localities prior  
195 to the Neoproterozoic, but there are too few of these from the limited relicts of pre-Neoproterozoic crust  
196 to be considered representative. In an Invited Centennial Article (Johnson and Brown, 2018), we  
197 used a dataset of 456 localities to investigate “*Secular change in metamorphism and the onset of*  
198 *global plate tectonics*”. This was followed by the 51<sup>st</sup> Hallimond Lecture of the Mineralogical  
199 Society of Great Britain and Ireland (Brown and Johnson, 2019), where we used an enlarged  
200 dataset of 564 localities to assess “*Time’s arrow, time’s cycle: Granulite metamorphism and*  
201 *geodynamics*.” In this final article of the series, we use the same dataset to evaluate key changes  
202 in the intensive variables of crustal metamorphism, particularly in relation to the appearance of  
203 dual tectono-thermal environments, and secular change in the evolution of subduction and  
204 collisional orogenesis since the Archean. We argue that it is the widespread appearance of dual  
205 tectono-thermal environments that is the critical evidence of a linked network of relatively  
206 narrow plate boundaries, which signifies the emergence of plate tectonics on Earth. Inevitably,  
207 there is some overlap between these articles, but each has a different orientation and goal, with  
208 the hope that the reader will find something novel and of interest in each.

209

210

## METHODS AND DATA ANALYSIS

211           The thermal history of the crust is stored in the metamorphic rock record (Brown and  
212 Johnson, 2018, 2019). At the present day, different tectonic settings along convergent plate  
213 boundaries exhibit contrasts in heat flow that are registered as differing metamorphic facies  
214 series in distinct crustal terranes (Miyashiro, 1961; Brown, 1998, 2006, 2010). Based on an  
215 extensive review of the literature on crustal metamorphism up to the end of February 2018, we  
216 have created a dataset of  $T$ ,  $P$ , thermobaric ratio ( $T/P$ ), and age ( $t$ ) of metamorphism for 564  
217 localities from the Cenozoic to the Eoarchean, although before the Neoproterozoic data are  
218 sparse (Brown and Johnson, 2018; dataset update of 28 February 2018 (Supplementary Data  
219 Table 1)).

220           We have restricted the dataset to crustal protoliths, so we do not include data from  
221 orogenic peridotites or data based on ultrahigh-pressure minerals in chromitites associated with  
222 ophiolitic complexes and in mantle xenoliths. The principal outputs that we use are quantitative  
223 estimates of the pressure ( $P$ ), temperature ( $T$ ), and age of metamorphism—all three must be  
224 available for a particular sample or locality to be included in the dataset. Our analysis relies on  
225 an assumption that the close-to-peak mineral assemblages are robust recorders of  $P$  and  $T$ . For  
226 this reason, the initial studies were limited to rocks equilibrated under conditions of relatively  
227 high temperature, such as granulites and eclogites (Brown, 2007, 2014), which are difficult to  
228 retrogress or overprint without fluid influx. In these early studies, for high-temperature  
229 metamorphism at  $P < 1$  GPa, a minimum temperature for inclusion was set at 700 °C, whereas  
230 for high-pressure metamorphism at  $T < 700$  °C a minimum pressure of 1 GPa was applied to  
231 ensure a reasonable minimum temperature and the likelihood of an equilibrated peak mineral

232 assemblage. In the data for the low T/P type metamorphism, a majority of the pressures are  
233 minima based on, for example, the presence of coesite relicts. Overall, about 30% of the low T/P  
234 metamorphic rocks in the dataset were interpreted to retain evidence of peak pressure whereas  
235 about 70% of the data represent the  $P$ – $T$  conditions at the maximum pressure retrieved, and  
236 therefore are minima (Supplementary Data Table 1).

237         We are cognizant that as methods improve progressively lower grade metamorphic rocks  
238 may be incorporated in the dataset, providing a reliable age for the peak metamorphism is also  
239 available. Thus, in the current dataset we include seven localities with  $T < 700$  °C in the high T/P  
240 type, eleven localities with  $P$  of 0.8–1.0 GPa in the intermediate T/P type, and one locality with  
241  $P < 1.0$  GPa in the low T/P type. Of the 223 high T/P type data, two localities are from well-  
242 known regional-scale UHT contact metamorphic aureoles (Rogaland in southern Norway and  
243 Makhavinekh Lake in eastern Canada). In addition, in low T/P type metamorphic rocks  
244 overprinted during exhumation, mineral indicators of close-to-peak pressures, such as coesite or  
245 diamond, are commonly preserved as inclusions in rock-forming or accessory minerals, which  
246 has proven to be important for retrieving minimum  $P$ – $T$  conditions from these rocks.

247         Thermobaric ratio is a more useful parameter than  $T$  or  $P$  because, on the contemporary  
248 Earth, each thermobaric type of metamorphism is associated with a particular plate tectonic  
249 setting. Insofar as metamorphic  $P$  can be translated to depth, the thermobaric ratio ( $T/P \sim T/z$ )  
250 can be viewed as a proxy for the transient geothermal gradient at the metamorphic peak. To  
251 highlight this relationship, discussions of earlier versions of this dataset (Brown, 2006, 2007,  
252 2014; Brown and Johnson, 2018) used the term “apparent thermal gradient.” However, as  
253 discussed more fully in Brown and Johnson (2019), we now prefer the term thermobaric ratio to  
254 avoid any possible confusion with the true geothermal gradient or the geotherm or the

255 metamorphic field gradient. Using thermobaric ratio ( $T/P$ ), metamorphic rocks are classified into  
256 three groups, which are based on the natural groups from Brown (2007) based on rock type (Fig.  
257 2): high  $T/P$  type ( $>775$  °C/GPa, arithmetic mean  $\sim 1100$  °C/GPa;  $n = 223$ ), including common  
258 and ultrahigh temperature (UHT) granulites; intermediate  $T/P$  type ( $775\text{--}375$  °C/GPa, arithmetic  
259 mean  $\sim 580$  °C/GPa;  $n = 152$ ), including high pressure (HP) granulites and medium or high  
260 temperature (medium- $T$ /high- $T$ ) eclogites; and, low  $T/P$  type ( $<375$  °C/GPa, arithmetic mean  
261  $\sim 250$  °C/GPa;  $n = 189$ ), including blueschists and low-temperature (low- $T$ ) eclogites, and  
262 ultrahigh pressure (UHP) metamorphic rocks.

263 Plots of  $T$  and  $P$  versus age are provided in Supplementary Figures 1 and 2<sup>1</sup>, respectively;  
264 secular change in the  $T$  and  $P$  of metamorphism was discussed recently by Brown and Johnson  
265 (2019), and is not reiterated here. A histogram and probability density function (PDF) curve for  
266 the age of metamorphism for the 564 localities used in this study are provided in Supplementary  
267 Figure 3<sup>1</sup>. Such analysis demonstrates the close association between crustal metamorphism and  
268 the supercontinent cycle, which has been recognized for more than a decade (Brown, 2007).

269 In this study, we concentrate on the petrogenesis of low and intermediate  $T/P$   
270 metamorphic rocks and their relationship to subduction at convergent plate boundaries and in  
271 collisional orogenesis. We begin by discussing whether the metamorphic conditions preserved by  
272 low  $T/P$  oceanic rocks correspond to subduction zone thermal gradients. We then critically assess  
273 two topical issues relating to subduction-related metamorphism: whether the formation of  
274 lawsonite requires abnormally low thermal gradients; and, whether oceanic subduction-related  
275 rocks register significantly lower maximum pressures than continental subduction-related rocks,  
276 and by implication had different mechanisms of exhumation. Finally, we discuss several key  
277 changes in crustal metamorphism through time that are revealed by a plot of  $T/P$  from

278 metamorphic rocks grouped by type plotted against age (Fig. 3); these data are also shown on a  
279 series of four maps to demonstrate the spatial relationships between the different types of  
280 metamorphism (Supplementary Figure 4<sup>1</sup>). These are: (1) the widespread appearance of low  $T/P$   
281 metamorphism during the Neoproterozoic, which is interpreted as evidence of cold collision and  
282 deep continental subduction; (2) the rare occurrence of low  $T/P$  metamorphism in the  
283 Paleoproterozoic, which may be evidence of atypical localized regions of cold collision; and, (3)  
284 the widespread appearance of dual high and intermediate  $T/P$  type metamorphism at the  
285 beginning of the Neoproterozoic, which may manifest the stabilization of subduction and the  
286 emergence of plate tectonics by the late Archean–early Proterozoic.

287

## 288 **LOW $T/P$ METAMORPHISM AND SUBDUCTION**

289 If we are to use the  $P$ – $T$  conditions retrieved from low  $T/P$  metamorphic rocks to  
290 understand tectonics, it is clearly important to know how these data relate to the  $P$ – $T$  conditions  
291 associated with active subduction of oceanic lithosphere. However, it turns out that this is a  
292 controversial issue. In a recent study it was argued that “*(thermal) models (of subduction) predict*  
293 *temperatures that are on average colder than those recorded by exhumed rocks*”, and further  
294 “*that exhumed high- $P$  rocks provide a more accurate constraint on  $P$ – $T$  conditions within*  
295 *subduction zones, and that those conditions may closely represent the subduction geotherm*”  
296 (Penniston-Dorland et al., 2015; note that these authors define the subduction geotherm as “*the*  
297  *$P$ – $T$  distribution along the subducting slab top*”). In addition, Penniston-Dorland et al. (2015)  
298 argued that the next generation of thermal models should more comprehensively incorporate all  
299 sources of heat, with a particular emphasis on shear heating as the most likely missing  
300 contribution to the heat budget. However, van Keken et al. (2018) have recently addressed this

301 issue and have argued that the discrepancy between models and rocks is beyond what can be  
302 explained by inclusion in the models of additional sources of heat, such as shear heating. They  
303 find that the addition of reasonable amounts of shear heating leads to a temperature rise of  $<50^{\circ}\text{C}$   
304 in the oceanic crust compared to models that exclude this heat source (cf. Abers et al., 2017;  
305 Maunder et al., 2018). Therefore, to explain the discrepancy these authors argued that “*typical*  
306 *blueschists and eclogites were exhumed preferentially under relatively warm conditions that*  
307 *occurred due to the subduction of young oceanic lithosphere or during the warmer initial stages*  
308 *of subduction*” (cf. Abers et al., 2017).

309 In their study, Penniston Dorland et al. (2015) did not distinguish between continental  
310 and oceanic low T/P metamorphic rocks. Nearly half of the low T/P metamorphic rocks for  
311 which we have  $P$ – $T$  and age information are continental in origin (Supplementary Data Table<sup>1</sup>),  
312 and represent subduction of arc or continental ribbon terranes, or subduction of the leading edge  
313 of a continent during collisional orogenesis. Given the potential for slab breakoff as the buoyant  
314 continental crust it is subducted to mantle depths and its intrinsic higher heat production, it may  
315 not be reasonable to expect a relationship between the peak  $P$ – $T$  conditions of continental rocks  
316 subsequently exhumed from mantle depths and the thermal gradients associated with active  
317 subduction of oceanic lithosphere.

318 To assess whether the peak  $P$ – $T$  conditions retrieved from low T/P continental  
319 metamorphic rocks are consistent with those from low T/P oceanic metamorphic rocks, in Figure  
320 4 we show a comparison between the thermal models of van Keken et al. (2018) for 56 present-  
321 day active subduction zones and peak  $P$ – $T$  conditions of low T/P metamorphic rocks from this  
322 study (Supplementary Data Table<sup>1</sup>) separated into continental ( $n = 84$ ) and oceanic ( $n = 105$ ).  
323 There is reasonable correspondence between the metamorphic data and the range of modeled

324 slab  $P$ – $T$  paths for the uppermost oceanic crust, but the correspondence is not as good for those  
325 for the lowermost oceanic crust (Fig. 4a). Also, the correspondence is poor for the  $P$ – $T$   
326 conditions averaged over the oceanic crust for each model and the overlap is biased towards the  
327 warmer active subduction zones (Fig. 4b).

328 In Figure 4c and d we show a third degree (cubic) polynomial regression through each of  
329 the oceanic and continental data to facilitate a more appropriate comparison with the thermal  
330 models. There is a relatively poor correspondence between the regression through the  $P$ – $T$   
331 conditions retrieved from low  $T/P$  metamorphic rocks of continental affinity and the average  $P$ – $T$   
332 conditions of the 56 models for the uppermost oceanic crust (Fig. 4c). Unsurprisingly, consistent  
333 with the comparison between the data and the individual models, the correspondence is worse for  
334 the average of the 56 models of  $P$ – $T$  conditions averaged over the oceanic crust (Fig. 4d).

335 However, for low  $T/P$  metamorphic rocks of oceanic affinity, an *a priori* premise that they may  
336 closely represent the model subduction  $P$ – $T$  paths might be plausible. Indeed, there is a striking  
337 similarity in shape between the regression through the  $P$ – $T$  conditions retrieved from low  $T/P$   
338 metamorphic rocks of oceanic affinity and the average  $P$ – $T$  conditions of the 56 models for the  
339 uppermost oceanic crust, although the rock-based regression is offset to higher  $T$  (by ~100–150  
340 °C) and/or lower  $P$  (by ~0.5–1.0 GPa; Fig. 4c). This is significantly larger than the offset  
341 expected from the effects of shear heating (Van Keken et al., 2018; Abers et al., 2017; Maunder  
342 et al., 2018). As we might expect, the rock-based regression has larger offsets to higher  $T$  and/or  
343 lower  $P$  when compared with the average of the 56 models of  $P$ – $T$  conditions averaged over the  
344 whole oceanic crust (Fig. 4d).

345 For low  $T/P$  metamorphic rocks of oceanic affinity, one simple interpretation of these  
346 relationships is that they were preferentially exhumed under warmer than average conditions and

347 from the uppermost several kilometers of oceanic crust. However, the rare occurrence of  
348 eclogites with gabbro protoliths in some low T/P metamorphic terranes, such as the Ligurian  
349 meta-ophiolites, Italy (Piccardo et al., 2002), and the Zermatt-Saas ophiolite, Switzerland  
350 (Angiboust et al., 2009), may suggest that this interpretation does not apply to all low T/P  
351 metamorphic rocks of oceanic affinity.

352 We note that there are various factors that affect the slab temperature in the models,  
353 including the age and speed of the incoming plate, and the dip of the slab (Maunder et al., 2018).  
354 In the slab above the decoupling depth, slab temperature is dependent on the age, whereas below  
355 this depth slab temperature is dependent on the speed, with slower slabs being hotter; varying the  
356 decoupling depth from 40 to 100 km also has an effect of the temperatures in the slab crust  
357 (Maunder et al., 2018). Furthermore, within the topmost kilometer or two of the slab, faster slabs  
358 may have hotter tops due to more vigorous convection in the mantle wedge (Magni et al., 2014).  
359 Thus, the relationship between  $P$ - $T$  data retrieved from exhumed low T/P metamorphic rocks  
360 and  $P$ - $T$  paths determined from slabs in thermal models of subduction is not going to be  
361 straightforward.

362 The implication of the van Keken et al. (2018) study is that the discrepancy between the  
363  $P$ - $T$  conditions retrieved from rocks and those in the thermal models is that the former are  
364 anomalous and do not relate to steady-state subduction. However, do the retrieved  $P$ - $T$   
365 conditions represent the peak  $P$ - $T$  conditions? Uncertainties associated with thermobarometry  
366 have been discussed in detail by Powell and Holland (2008). In general, we concur with  
367 Penniston-Dorland et al. (2015) that systematic errors in the  $P$ - $T$  determinations are unlikely.  
368 However, we posit that the discrepancy may be related in part to underestimation of the peak  
369 pressure attained by low T/P metamorphic rocks. As discussed above, for the low T/P type



370 metamorphism about 70% of the pressures are based on minima, for example, the presence of  
371 coesite relicts. Furthermore, in eclogites in particular, the mineral assemblages are commonly  
372 high-variance. Phase equilibrium modeling of such assemblages generally predicts large stability  
373 fields in which the abundance and composition of minerals show little change, features that do  
374 not permit tight constraints on either  $P$  or  $T$ . For similar reasons, the application of conventional  
375 thermobarometry to such rocks is also problematic. These problems have been discussed recently  
376 with respect to the intragranular coesite eclogites at Yangkou Bay in the Sulu belt, where it has  
377 been shown that  $P$ – $T$  conditions were significantly underestimated in previous studies (Xia et al.,  
378 2018)—this may be true for other localities.

379       Leaving aside the discussion about possible underestimation of pressure, and taking the  
380 data at face value, oceanic low T/P metamorphic rocks with  $P_{\max} < 2.2$  GPa lie at pressures  
381 below a majority of the  $P$ – $T$  paths for both uppermost oceanic crust and those averaged over the  
382 oceanic crust (Fig. 4), which means their  $P$ – $T$  conditions are too ‘warm’ to have been formed and  
383 exhumed in most of the relatively ‘cool’ subduction environments active on Earth at the present  
384 day. However, rocks with  $P_{\max} > 2.5$  GPa overlap the full range of  $P$ – $T$  paths for the uppermost  
385 oceanic crust in Figure 4a, and could be evidence of exhumation related to a wide range of  
386 subduction zone tectono-thermal environments.

387       To address this possibility more fully, in Figure 5 we show a comparison between three  
388 exemplar thermal models for the top of the ocean crust that are representative of warm,  
389 intermediate and cold subduction, respectively, from initiation to 30 Ma (van Keken et al., 2018),  
390 together with peak  $P$ – $T$  conditions of oceanic low T/P metamorphic rocks. Although all of the  
391 oceanic low T/P metamorphic rocks could be explained by preferential exhumation under  
392 relatively warm conditions (Fig. 5a), because all lie at  $P$ – $T$  conditions within the slab (i.e. on  $P$ – $T$

393 paths cooler than those shown for the top of the ocean crust in Fig. 5a), this is only a requirement  
394 for a minority of the data. This is demonstrated by Figures 5b and c, where only 30% of the data  
395 plot at  $P < 2.2$  GPa and, therefore, lie at  $P$ - $T$  conditions outside the slab for colder subduction  
396 (i.e. on  $P$ - $T$  paths that are warmer than those shown for the top of the ocean crust). Another  
397 ~30% of the data, those at  $P > 2.5$  GPa, could have been exhumed from the oceanic crust under  
398 any thermal conditions, because these data all lie at  $P$ - $T$  conditions within the slab for all three  
399 exemplar thermal models, as shown in Figure 5 (i.e. on  $P$ - $T$  paths that are cooler than those  
400 shown for the top of the ocean crust in all three examples).

401         The remaining ~40% of the data lie within a pressure range that corresponds to the  
402 assumed depth at which the behavior between the slab and the overriding plate and/or mantle  
403 wedge changes from decoupled (at lower  $P$ ) to coupled (at higher  $P$ ) in the thermal models of  
404 van Keken et al. (2018). At depths of 75 to 80 km, as the slab begins to couple with the  
405 overriding mantle of the wedge, corner flow draws hotter mantle from beneath the arc-backarc  
406 system into the wedge, warming the down going oceanic lithosphere. This correspondence  
407 suggests a possible relationship between the change from decoupling to coupling along the  
408 subduction interface and the exhumation of these intermediate pressure low T/P metamorphic  
409 rocks. Although the depth at which a subducting slab becomes coupled to the mantle wedge may  
410 depend on a variety of parameters, a depth of 70–80 km appears to be a robust result (Wada and  
411 Wang, 2009) and the correspondence is probably not simply a coincidence.

412         Lastly, we address the issue of secular cooling of the mantle. In Figure 6 we show a  
413 comparison between model slab  $P$ - $T$  paths for the uppermost and lowermost oceanic crust from  
414 the thermal models of van Keken et al. (2018) for 56 present-day active subduction zones  
415 calculated for mantle  $T_P$  of 1350 °C, 1420 °C, 1500 °C and 1570 °C (P. Van Keken, January

416 2019, unpublished), and peak  $P$ – $T$  conditions of low  $T/P$  metamorphic rocks. The temperature  
417 rise from the lowest to the highest mantle  $T_P$  varies with depth, being 10–50 °C at 30 km, 20–70  
418 °C at 60 km, 90–130 °C at 90 km and 80–120 °C at 120 km for the uppermost oceanic crust (the  
419 rise is similar for the lowermost oceanic crust). Overall, there is no apparent relationship between  
420 the age of low  $T/P$  metamorphism of oceanic rocks and the range of subduction zone tectono-  
421 thermal environments that might reflect secular cooling. This may not be surprising since the  
422 decrease in average mantle  $T_P$  since the beginning of the Neoproterozoic—likely <100 °C—  
423 approximates the probable range of mantle  $T_P$  (assumed to have been similar to the estimate of  
424 ~120 °C for MORB; Herzberg et al., 2007). Furthermore, even at mantle  $T_P$  much higher than  
425 expected for the Neoproterozoic (1500 and 1570 °C; Fig. 6 c,d), it remains difficult to explain  
426 oceanic low  $T/P$  metamorphic rocks with  $P_{\max} < 2.2$  GPa other than by preferential exhumation  
427 under relatively warm conditions that occurred due to the subduction of young oceanic  
428 lithosphere or during the warmer initial stages of subduction.

429         In addition to factors that affect the model results, any interpretation of large datasets  
430 leads to generalized conclusions, whereas a balance among different processes will be important  
431 in the evolution of specific examples. As Agard et al. (2009) have shown in relation to the  
432 exhumation of oceanic low  $T/P$  metamorphic rocks, while the exhumation of some may be  
433 related to warm subduction, the exhumation of others was more likely related to processes such  
434 as continental subduction or a modification of the convergence vector (e.g., the velocity and/or  
435 angle of subduction) across the subduction zone. Overall, how  $P$ – $T$  data derived from exhumed  
436 metamorphic rocks might relate to the  $P$ – $T$  conditions associated with active subduction of  
437 oceanic lithosphere is a complex issue that is likely to be debated for a while before any  
438 acceptable resolution is achieved.

439

440 **WHY DO LOW T/P ROCKS ONLY APPEAR WIDELY IN THE GEOLOGICAL RECORD**  
441 **SINCE THE NEOPROTEROZOIC?**

442 Figure 7 shows the global distribution of low T/P metamorphic rocks. With a few  
443 exceptions, these localities are younger than Tonian (<0.72 Ga) in age (Fig. 3; Supplementary  
444 Data Table<sup>1</sup>). Three main hypotheses have been proffered to explain why blueschists in  
445 particular are largely absent from the rock record prior to the late Neoproterozoic, but arguments  
446 for the absence of blueschists also apply to low T/P rocks in general.

447 In a landmark paper concerned with the production and preservation of blueschist and  
448 low-T eclogite facies metamorphic rocks, England and Richardson (1977) proposed that  
449 blueschist mineral assemblages were overprinted during exhumation and/or blueschists were  
450 removed from the rock record by erosion. These authors envisaged a thick wedge of cold  
451 sediments overlying oceanic lithosphere or a continental margin that was loaded during  
452 subduction and terminal collision. They argued that as pressure decreased due to erosion so  
453 thermal relaxation would lead to an increase in temperature for a time determined by the initial  
454 depth. For this type of *P–T* evolution of low T/P terrains, the increase in temperature will lead to  
455 the production of rocks with mineral assemblages characteristic of higher *T/P* greenschist,  
456 amphibolite or granulite facies. For a reasonable erosional time constant of 200 Ma, England and  
457 Richardson (1977) were able to show that blueschists would be expected at the surface at 50–100  
458 Ma after the termination of subduction, and, furthermore, that continued erosion of such belts for  
459 several hundred million years would significantly reduce the probability of blueschist  
460 preservation.

461           Although the timescales of overprinting and complete loss by erosion are functions of  
462 assumptions made in the modeling, the predictions of the model are broadly supported by the  
463 observation that most Precambrian low T/P localities are represented by HP metamorphic rocks,  
464 commonly eclogites, within terranes that have been severely overprinted during exhumation  
465 (Carlson et al., 2007; Weller and St-Onge, 2017; Xu et al., 2018). This may imply that any  
466 blueschists that may have been produced were removed by erosion leaving behind only the  
467 strongly retrogressed medium-T/high-T eclogites.

468           As an alternative to removal by erosion, Brown (2006) postulated that secular cooling of  
469 the upper mantle led to increasingly stronger lithosphere that, by the late Tonian, enabled deep  
470 subduction of continents, deeper slab breakoff and formation and preservation of blueschists and  
471 low-*T* eclogites during collisional orogenesis. This hypothesis has been tested for a range of  
472 conditions using a 2-D petrological–thermomechanical numerical model (Sizova et al., 2012,  
473 2014). Based on a series of experiments, Sizova et al. (2012, 2014) proposed that an increase of  
474 the ambient upper-mantle temperature to >80–100 °C higher than the present-day value,  
475 corresponding to the early Neoproterozoic, leads to modes of collision that differ from the  
476 modern tectonic regime. In particular, dehydration of the subducting slab and high fluid pressure  
477 weaken the overriding plate, which undergoes extension associated with decompression partial  
478 melting of the mantle wedge. Early during the collision, conductive heating of the subducting  
479 slab by the hot asthenosphere of the wedge weakens the slab, causing shallow breakoff, which  
480 localizes at the ocean–continent transition at a depth of ~100 km. In these circumstances the  
481 formation and preservation of low T/P metamorphic rocks during collisional orogenesis does not  
482 occur, consistent with the geological record.

483           Recently it was proposed that sodic amphibole (and blueschists) became more prevalent,  
484 in particular since the late Precambrian, due to secular change in the composition of oceanic  
485 crust, which became less magnesian due to a decrease in mantle melting as a consequence of  
486 secular cooling (Palin and White, 2016). This hypothesis is based on the calculated  $P$ – $T$  stability  
487 of sodic amphibole, which is stable in MgO-poor ( $\leq 11.2$  wt%) compositions, but is not predicted  
488 to form in higher-MgO rocks under low thermal gradients (Palin and White, 2016). However,  
489 there is a wide range of basalt compositions in ancient greenstone belts, including more than half  
490 with MgO-poor ( $\leq 11.2$  wt%) compositions (dataset of Condie et al., 2016;  $n = 3414$  samples). If  
491 tectonic settings that could have generated low thermal gradients were widespread during the  
492 Precambrian, blueschists would be expected to have formed, although it remains an open  
493 question whether they would have been preserved and exhumed. Thus, if they formed, the  
494 absence of blueschists prior to the late Tonian is less likely due to an absence of suitable rock  
495 compositions and more likely due to a preservation/exhumation bias related to the change from  
496 warm to cold collisional orogenesis during the late Precambrian (Sizova et al., 2012, 2014).

497           We can further examine the possibility that rock compositions limit the appearance of  
498 low  $T/P$  mineral assemblages by using the metamorphic facies concept. This fundamental  
499 concept in petrology is based on the observation that, within a limited range of  $P$ – $T$  conditions,  
500 there is an inevitable relation between the mineral assemblage and chemical composition of a  
501 rock—if we know the chemical composition of the protolith, we can predict the corresponding  
502 mineral assemblage at any  $P$ – $T$  condition (Fyfe and Turner, 1966; Turner, 1968). This  
503 relationship between the range of possible chemical compositions and the set of predicted  
504 mineral assemblages is immutable.

505 Clearly, the the metamorphic facies concept cannot be affected by secular change in the  
506 composition of rocks. Thus, recent suggestions that secular change in the composition of shales,  
507 greywackes and basalts may limit the application of the metamorphic facies concept to rocks of  
508 Archean age (Nicoli and Dyck, 2018; Palin and Dyck, 2018) are misleading. Given knowledge  
509 of the range of protolith compositions, and applying quantitative metamorphic petrology, the  
510 facies concept allows us to predict what mineral assemblages will be stabilized under low  $T/P$   
511 metamorphic conditions from the earlier rock record, particularly Archean greenstone belts. Such  
512 an approach would help us as a community to meet the challenge posed by Ganne et al. (2012)  
513 that the apparent scarcity of old blueschist facies series metamorphism is most likely due to a  
514 methodological problem in deciphering the  $P-T$  evolution within greenstone belts rather than a  
515 result of poor preservation or absence.

516

517 **ARE RARE OCCURRENCES OF LOW  $T/P$  METAMORPHISM IN THE**  
518 **PALEOPROTEROZOIC EVIDENCE OF ATYPICAL LOCALIZED REGIONS OF COLD**  
519 **COLLISION OR SOMETHING MORE?**

520 One notable feature of the Paleoproterozoic Era is the occurrence of several localities  
521 that record low  $T/P$  thermobaric ratios comparable to rocks preserved and exhumed in  
522 Phanerozoic collisional orogens (Fig. 3; Supplementary Data Table<sup>1</sup>). These data have been used  
523 to suggest that subduction-related processes similar to those active on the contemporary Earth  
524 may have been operative during the Paleoproterozoic Era (Ganne et al., 2012; Weller and St-  
525 Onge, 2017; Glassley et al., 2014; Xu et al., 2018). For example, the preferred geodynamic  
526 model for the early Palaeoproterozoic tectonic evolution of greenstone belts in the West African  
527 craton involves supracrustal rocks metamorphosed under low  $T/P$  conditions in an accretionary

528 prism followed by extrusion by buoyancy flow during ongoing subduction (Ganne et al., 2012).  
529 Similarly,  $P$ – $T$  conditions retrieved from an eclogite xenolith in Paleoproterozoic carbonatite at  
530 the western edge of the Trans North China orogen were used to argue for cold subduction as  
531 early as 1.8 Ga (Xu et al., 2018).

532         However, the similarity is particularly compelling in the case of the Trans-Hudson  
533 orogen, which has been considered as an ancient example of a Himalayan-type continental  
534 collision (St-Onge et al., 2006). In this interpretation, the upper plate comprises the Rae and  
535 North Atlantic cratons, which are sutured by various Paleoproterozoic belts (St-Onge et al.,  
536 2009), including the Nagsugtoqidian orogen in southern West Greenland, where low  $T/P$   
537 metamorphic rocks have been retrieved from the suture of a continent–continent collision zone  
538 (Glassley et al., 2014). The lower plate is represented by the Superior craton on the southern side  
539 of the Trans-Hudson orogen in Canada. Therefore, the inferred Paleoproterozoic upper plate is  
540 considered to occupy the same position as south-east Asia in the Cenozoic prior to the collision  
541 of India with the Lhasa block along its southern margin. In this context, the low  $T/P$  eclogite in  
542 the Kovik tectonic window in the Trans-Hudson orogen is considered analogous to the non-  
543 coesite-bearing portions of the Tso Morari eclogite massif in the Himalayas (Weller and St-  
544 Onge, 2017).

545         There is a range of contemporary mantle  $T_P$  of  $\sim 120$  °C (Herzberg et al., 2007), which  
546 suggests that the mantle is not in an end-member thermally well-mixed regime, but may be  
547 closer to a thermal isolation regime, which is characteristic when a subduction zone girdle  
548 surrounds a supercontinent (Lenardic et al., 2011). Assuming a similar range of mantle  $T_P$  in the  
549 past, as suggested by the data shown in Fig. 1 (Supplementary Data Table<sup>1</sup>), then different styles  
550 of Proterozoic orogenic belt might be anticipated according to the variation in mantle  $T_P$ . For



551 example, orogens related to closing of an internal ocean within the supercontinent subduction  
552 girdle would have been associated with higher mantle  $T_P$ , whereas those associated with  
553 elimination of a segment of an external ocean outside the supercontinent subduction girdle would  
554 have been associated with lower mantle  $T_P$ .

555 In this wider context, we consider the Paleoproterozoic localities that record low  $T/P$   
556 thermobaric ratios could represent atypical localized regions on Earth where the style of  
557 subduction and collision was similar to modern tectonic environments, rather than being  
558 representative of the dominant subduction and collisional style prevalent during the  
559 Paleoproterozoic Era. For example, if the incoming oceanic lithosphere that was being subducted  
560 in these cases represented segments of an external ocean related to a supercraton, the subducting  
561 slabs could have been relatively old and cold, which would have skewed their thermal structure  
562 to low temperatures. Interestingly, in the interpretation of Pehrsson et al. (2013), for the Trans-  
563 Hudson orogen the upper plate cratons were derived from the supercraton Nunavutia whereas the  
564 lower plate Superior craton was derived from the supercraton Superia, suggesting the possibility  
565 of an old and cold superocean separating them that could have been subducted during the  
566 convergence and collision. This prediction will be tested over time. In addition, if more data of  
567 low  $T/P$  type are discovered from a wider range of localities from different Precambrian orogenic  
568 belts, these conclusions may need to be revisited.

569

## 570 **OTHER ISSUES RELATED TO LOW $T/P$ METAMORPHISM**

### 571 **Does the formation of lawsonite require abnormally low thermal gradients?**

572 It has been argued that lawsonite-bearing low  $T/P$  type metamorphic rocks preserve  
573 evidence of very low temperature conditions in subduction zones, that is that their formation

574 requires abnormally low thermal gradients of less than approximately 250 °C/GPa (Tsujimori et  
575 al., 2006). Our analysis of  $P$ – $T$  data from 189 localities with low  $T/P$  metamorphic rocks  
576 demonstrates that lawsonite-bearing metamorphic rocks ( $n = 45$ ; 1 outlier excluded) have a mean  
577  $T/P$  of  $236 \pm 64$  ( $1\sigma$ ) °C/GPa, with a range of 155–357 °C/GPa, whereas lawsonite-absent low  
578  $T/P$  metamorphic rocks ( $n = 143$ ) have a mean  $T/P$  of  $260 \pm 59$  ( $1\sigma$ ) °C/GPa, with a range of  $T/P$   
579 = 133–393 °C/GPa (Fig. 8a). Thus, there is no significant difference in thermal gradients  
580 between Lws-bearing and Lws-absent metamorphic rocks. This outcome may not be surprising  
581 since lawsonite occurs in low  $T/P$  type metamorphic rocks of both continental and oceanic  
582 affinity (Supplementary Data Table<sup>1</sup>).

583         Based on phase equilibrium modeling, and assuming fluid-saturated conditions, lawsonite  
584 eclogite and blueschist are expected to be the dominant rock types that form during subduction  
585 of oceanic crust, and therefore it might be expected that they would be abundant in exhumed  
586 subduction complexes (Wei and Clarke, 2011). What then is the explanation for the relative  
587 scarcity of lawsonite in the rock record? There are multiple reasons. Since the quantity of H<sub>2</sub>O  
588 required to saturate the phase assemblage increases into the lawsonite stability field (Weller et  
589 al., 2015, Fig. 6d), a low initial H<sub>2</sub>O content in the protolith would have limited the amount of  
590 lawsonite in the mode, making it vulnerable to retrograde loss during exhumation, perhaps  
591 without leaving sufficient microstructural evidence of its former presence. The sparse abundance  
592 could also have been related to dehydration during subduction prior to reaching the lawsonite  
593 stability field, such that the rock became H<sub>2</sub>O undersaturated, precluding the formation of  
594 lawsonite (Clarke et al., 2006). In addition, as shown in Figure 8a, the stability limit of  
595 lawsonite-bearing rocks has a steep slope in  $P$ – $T$  space and any of these rocks that were exhumed  
596 along decompression  $P$ – $T$  paths will likely be strongly retrogressed. Thus, in some cases, the

597 scarcity of lawsonite may simply be due to extensive retrogression during exhumation (e.g. Zack  
598 et al., 2004). This is a common problem that affects many eclogites for which the exhumation  $P$ -  
599  $T$  paths are not as cold as the prograde  $P$ - $T$  paths and, in the case of rocks with lawsonite,  
600 breakdown will be accompanied by the release of a large amount of structurally-bound fluid to  
601 promote retrogression (Wei and Clarke, 2011).

602

### 603 **Is there a difference in $P_{\max}$ between oceanic and continental low T/P metamorphic rocks?**

604 Next we examine the postulate that oceanic subduction-related rocks record lower  $P_{\max}$   
605 ( $<2.3$  GPa, Agard et al., 2009;  $<2.7$  GPa, Erdman and Lee, 2014) than continental subduction-  
606 related rocks ( $>2.7$  GPa) that may also have slightly higher prograde thermal gradients (Erdman  
607 and Lee, 2014), suggesting that the mechanism and pathways of their exhumation likely differ.  
608 Oceanic and continental low T/P metamorphic rocks yield a similar range of thermobaric ratios  
609 (Fig. 8b). A histogram of  $P_{\max}$  values for oceanic low T/P metamorphic rocks ( $n = 104$ ; 1 outlier  
610 excluded) and continental low T/P metamorphic rocks ( $n = 84$ ) is shown in Figure 8c. This figure  
611 shows that there is very little difference in  $P_{\max}$  values between oceanic and continental low T/P  
612 metamorphic rocks, which is confirmed by the mean  $P$  of  $2.38 \pm 0.88$  ( $1\sigma$ ) GPa with a range of  $P$   
613 from 1.0 to 7.0 GPa for oceanic rocks compared to the mean  $P$  of  $2.99 \pm 1.04$  ( $1\sigma$ ) GPa with a  
614 range of  $P$  from 1.1 to 7.0 GPa for continental rocks. It is unclear whether these data inform us  
615 about general differences in exhumation processes in circumstances where the range of possible  
616 exhumation mechanisms is large (Agard et al., 2009; Kylander-Clark et al., 2012; Sizova et al.,  
617 2012; Hacker et al., 2013; Warren, 2013; Malusà et al., 2015).

618

### 619 **WHEN AND HOW DID PLATE TECTONICS EMERGE ON EARTH?**

620 “ . . . *the existence of a local zone of tectonic divergence, lateral shear and/or*  
621 *convergence is not the same as the existence of plate tectonics . . . subduction is a*  
622 *component of plate tectonics but subduction does not constitute a plate tectonic planet.*”

623 (Lenardic, 2018, p. 4).

624

625 There are two significant changes in the metamorphic record, discussed in reverse order.  
626 First, during the Neoproterozoic, low T/P metamorphism became widespread in the rock record,  
627 mostly preserved in sutures associated with late Neoproterozoic and Phanerozoic collisional  
628 orogens, particularly in Eurasia (Figs 3, 7). This change has been interpreted as evidence of an  
629 evolution to stronger slabs, deeper slab breakoff and colder collisional orogenesis related to  
630 secular cooling of the mantle (van Hunen and van den Berg, 2008; van Hunen and Allen, 2011;  
631 Sizova et al., 2014). More important to the discussion here is an earlier change, in the  
632 Neoproterozoic, when there was an appreciable increase in the number of localities where evidence  
633 of high or intermediate T/P metamorphism was preserved (Fig. 3; Supplementary Figure 4<sup>1</sup>).  
634 This change has been interpreted as evidence of the stabilization of subduction and widespread  
635 collisional orogenesis to create the supercratons (Brown and Johnson, 2019). Thus, the  
636 Neoproterozoic likely records the completion of a globally-linked network of narrow plate  
637 boundaries and the emergence of plate tectonics.

638 In addition to these two singular changes, there is a gradual secular evolution in the  
639 pressure of intermediate T/P metamorphism, which on average has increased by ~0.25 GPa from  
640 the Neoproterozoic to the Neoproterozoic (Supplementary Figure 2). This increase of pressure  
641 through time is consistent with the prediction by Rey and Coltice (2008) that elevation of  
642 collisional orogens is expected to have increased through the Proterozoic. In Figure 9a we show

643 all  $T/P$  data for the period from 4.0 Ga to the present day, contoured for density. As the low  $T/P$   
644 data swamp the Precambrian data in Figure 9a, we also show in Figure 9b the  $T/P$  data for the  
645 period from 4.0 Ga to 0.85 Ga, contoured for density. These plots emphasize the gradual  
646 evolution of bimodality in type of metamorphism during the Proterozoic, consistent with secular  
647 change in mantle  $T_P$  in a plate tectonics regime that emerged on Earth in the Neoproterozoic.

648 In Figure 10 we plot histograms of ages, probability density functions and cumulative  
649 smooth kernel density estimates for low  $T/P$  and intermediate  $T/P$  type metamorphism. These  
650 data clearly define three principal periods of activity increasing in magnitude from the first at  
651  $>2.3$  Ga, to the formation of Columbia at c. 2.2 to 1.8 Ga, to the breakup of Rodinia and the  
652 period of intense terrane tectonic activity since 0.8 Ga. These three periods of enhanced tectonic  
653 activity are separated first by the Palaeoproterozoic tectono-magmatic lull at 2.3–2.2 Ga  
654 (Spencer et al., 2018) and second by the boring billion from c. 1.8–1.7 to c. 0.8–0.7 Ga (Holland,  
655 2006; Cawood and Hawkesworth, 2014).

656 Interestingly, the first ( $>2.3$  Ga) period of enhanced tectonic activity follows a regional  
657 glaciation in the late Mesoarchean, evidence of which is preserved in South Africa (Young et al.,  
658 1998), and the rise of continents above sea level (Flament et al., 2008; Korenaga et al., 2017;  
659 Bindeman et al., 2018). In addition, the second (c. 2.2–1.8 Ga) and third ( $<0.8$  Ga) periods of  
660 enhanced tectonic activity follow ‘snowball’ Earth glaciations at 2.45–2.22 Ga and 0.75–0.63  
661 Ga, respectively (Gumsley et al., 2017; Hoffman, 2013; Hoffman and Schrag, 2002). Noting  
662 these correlations, Sobolev and Brown (2019) have proposed that major surface erosion events  
663 following snowball Earth glaciations increased the availability of sediment at continental edges  
664 to lubricate subduction, as indicated by the zircon oxygen isotope record (Spencer et al., 2014),  
665 which facilitated the Paleoproterozoic and Phanerozoic cycles of amplified plate tectonic activity

666 leading to the formation of Columbia and, after the boring billion, the ‘modern’ regime of terrane  
667 tectonics (Fig. 10). Furthermore, these authors argued that the rise of continents above sea level  
668 and the availability of sediments at the newly exposed continental edges allowed plate tectonics  
669 to emerge in the Neoproterozoic.

670         The change to a plate tectonic regime was likely gradual (Condie, 2018) and was broadly  
671 related to secular cooling since the Mesoproterozoic (Sizova et al., 2010). How this transition  
672 occurred depends on the geodynamic regime that existed before the Neoproterozoic. Prior to 2.8 Ga  
673 the crust registers moderate thermobaric ratios in both ‘high-grade’ gneiss terranes and ‘low-  
674 grade’ greenstone belts, with only rare occurrences of high T/P metamorphism and sporadic  
675 examples of intermediate T/P metamorphism, although reliable quantitative data are limited.  
676 This pattern may be evidence of transient subduction without plate tectonics, for example in a  
677 squishy lithosphere tectono-magmatic regime in which occurrences of intermediate T/P  
678 metamorphism may represent a record of episodes of local subduction and plate collision (Sizova  
679 et al., 2015, 2018; Rozel et al., 2017). Another plausible tectonic activity in the Archean is a type  
680 of episodic lid overturn and resurfacing (O’Neill et al., 2007), where the oceanic lithosphere  
681 overturns are due to the special case of retreating large-scale subduction triggered by large  
682 impacts (O’Neill et al., 2017) or mantle plumes (Gerya et al., 2015). This type of retreating  
683 subduction could have formed regional cells with plate-like behavior complete with internal  
684 spreading and transform boundaries (Gerya et al., 2015). It is likely that the retreating slabs  
685 transported water into the upwelling asthenospheric mantle via the hydrated crust of the slabs,  
686 enabling a large volume of magma to be generated, which would have been an efficient way to  
687 have produced the early, more mafic continental crust. Multiple collisions between such cells  
688 could have formed protocontinents (Sobolev and Brown, 2019).



711 The crustal record of metamorphism suggests a gradual evolution of bimodality in the  
712 tectono-thermal environments related to subduction and collision on Earth since the Neoproterozoic  
713 (Fig. 9). This evolution involved a secular increase in the pressure of intermediate T/P  
714 metamorphism since the Neoproterozoic, the limited occurrence of low T/P metamorphism in the  
715 rock record in the mid-Paleoproterozoic and the widespread appearance of low T/P  
716 metamorphism in the rock record since the late Tonian. In these circumstances it seems unlikely  
717 that the rate of destruction of continental crust would have remained approximately constant  
718 since the beginning of the Proterozoic, as argued by Scholl and von Huene (2010), since higher  
719 mantle  $T_p$  in the past would have led to shallower slab breakoff, and probably lower rates of  
720 subduction erosion and higher rates of crustal foundering (Sizova et al., 2014, 2015; Chowdhury  
721 et al., 2017; Perchuk et al., 2018).

722 It is more difficult still to determine the processes responsible for crustal destruction in  
723 the Archean, because the geodynamic regime is uncertain. Before the emergence of plate  
724 tectonics, crustal downwellings were probably random small-scale features (Gerya, 2014) and  
725 although crust was destroyed by a variety of processes (Johnson et al., 2014; Sizova et al., 2015)  
726 the rate of destruction appears to have been low. Based on geochemical modeling, Dhuime et al.  
727 (2012) identify a marked decrease in the rate of net crustal growth at c. 3 Ga that may be linked  
728 to the emergence of plate tectonics and the introduction of higher rates of crustal destruction.  
729 Even though plate tectonics had emerged by the late Neoproterozoic–early Proterozoic, collisional  
730 orogenesis was likely different than today and crustal recycling at these locations may have been  
731 achieved principally by peeling-off of dense lower continental crust and its return to the mantle  
732 (Chowdhury et al., 2017; Perchuk et al., 2018).



733 Cawood and Hawkesworth (2019) have argued that the area of continental crust reached  
734 a dynamic equilibrium of ~40% of the Earth's surface by the Mesoarchean, although they argue  
735 for a crust that was more mafic in composition and thinner than the present day prior to the  
736 Neoproterozoic. Furthermore, these authors have proposed that integration of thickness and area data  
737 suggests continental volume increased from the Hadean to the mid-Paleoproterozoic, but  
738 remained relatively constant in area and thickness through the boring billion (c. 1.8–1.7 Ga to  
739 0.8–0.7 Ga; Holland, 2006; Cawood and Hawkesworth, 2014). Then, in the mid-Neoproterozoic  
740 the rate of destruction began to exceed the rate of creation, perhaps due to increased rates of  
741 sediment subduction and subduction erosion related to the widespread appearance of low T/P  
742 metamorphism in the geological record.

743

744

#### CONCLUDING REMARKS

745 We finish by pointing out the principal shortcoming of our approach using the crustal  
746 record of metamorphism, which is clearly demonstrated by Figures 3 and 10. In common with  
747 other studies based on the continental rock record, the number of data available to us from before  
748 the Neoproterozoic are limited (Fig. 3) and, therefore, our summary of Earth's tectonic evolution  
749 only extends back to 3 Ga (Fig. 10). At present, the balance of geological evidence and the  
750 results of experiments run using numerical models of geodynamics indicate that subduction did  
751 not become stabilized until the late Mesoarchean, which, in turn allowed the emergence of plate  
752 tectonics by the late Archean–early Proterozoic. What is clear from the series of three articles we  
753 have written in the past year (Brown and Johnson, 2018, 2019, and this article) is that the overall  
754 pattern of the tectonic behavior of the Earth's lithosphere since the early Proterozoic is relatively  
755 well understood. What then are the priorities for future studies?

756 To better constrain the geodynamic regime in the early Earth, precedence should be given  
757 to recovery of  $P$ – $T$ –age data from a much larger number of localities in the Archean continental  
758 nuclei, particularly from the crust that predates the Neoproterozoic. This is imperative if we are to  
759 understand the transition from whatever tectonic mode operated on Earth prior to plate tectonics.  
760 The continued development of internally-consistent thermodynamic datasets and advances in the  
761 activity–composition models for phases of interest (Holland et al., 2011; White et al., 2014;  
762 Green et al., 2016; Holland et al., 2018), combined with advances in petrochronology (Engi et  
763 al., 2017), has provided us with the tools to apply quantitative petrology to a wide range of rock  
764 compositions and metamorphic grades in both greenstone belts and TTG gneiss terrains. Thus,  
765 this goal can be realized within the next few years by targeted studies based on new fieldwork  
766 combined with the use of legacy samples scattered in rock collections worldwide.

767 A second important consideration is to test the hypothesis implicit in this article that the  
768 rare occurrence of low  $T/P$  metamorphism in the Paleoproterozoic is evidence of atypical  
769 localized regions of cold collision. The four localities described to date (Ganne et al., 2012;  
770 Weller and St-Onge, 2017; Glassley et al., 2014; Xu et al., 2018) are intriguing, but do they  
771 imply that the global metamorphic rock record is skewed by overprinting and erosion (England  
772 and Richardson, 1977), and that the ‘modern’ regime (Fig. 10) featuring deep continental  
773 subduction began in the Paleoproterozoic? Time will tell.

774

775

#### ACKNOWLEDGEMENTS

776 The authors acknowledge discussions with Sarah Penniston-Dorland and Peter van Keken; we  
777 also thank Peter for providing the thermal models shown in Figs 4, 5 and 6. We are grateful for review  
778 comments from Nicolas Flament and Owen Weller, and editorial comments from Callum Hetherington,

779 which helped us to improve the content and presentation of this article. TEJ acknowledges support from  
780 Open Fund GPMR210704 from the State Key Laboratory for Geological Processes and Mineral  
781 Resources, China University of Geosciences, Wuhan. This article is a contribution to IGCP 648.

782

783

### ORCID

784 Michael Brown <http://orcid.org/0000-0003-2187-616X>

785 Tim Johnson <http://orcid.org/0000-0001-8704-4396>

786

787

### REFERENCES CITED

- 788 Abers, G.A., van Keken, P.E., and Hacker, B.R. (2017) The cold and relatively dry nature of mantle  
789 forearcs in subduction zones. *Nature Geoscience*, 10, 333–337.
- 790 Agard, P., Yamato, P., Jolivet, L., and Burov, E. (2009) Exhumation of oceanic blueschists and eclogites  
791 in subduction zones: timing and mechanisms. *Earth-Science Reviews*, 92, 53–79.
- 792 Angiboust, S., Agard, P., Jolivet, L., and Beyssac, O. (2009) The Zermatt-Saas ophiolite: the largest (60-  
793 km wide) and deepest (c. 70–80 km) continuous slice of oceanic lithosphere detached from a  
794 subduction zone? *Terra Nova*, 21, 171–180.
- 795 Arndt, N., and Davaille, A. (2013) Episodic Earth evolution. *Tectonophysics*, 609, 661–674.
- 796 Aulbach, S., and Arndt, N.T. (2019a) Eclogites as palaeodynamic archives: evidence for warm (not hot)  
797 and depleted (but heterogeneous) Archaean ambient mantle. *Earth and Planetary Science Letters*,  
798 505, 162–172.
- 799 Aulbach, S., and Arndt, N.T. (2019b) Origin of high-Mg bimineralic eclogite xenoliths in kimberlite –  
800 reply to comment from Claude Herzberg. *Earth and Planetary Science Letters*, 510, 234–237.
- 801 Bercovici, D., and Ricard, Y. (2014) Plate tectonics, damage and inheritance. *Nature*, 508, 513–516.

- 802 Bindeman, I.N., Zakharov, D.O., Palandri, J., Greber, N.D., Dauphas, N., Retallack, G.J., Hofmann, A.,  
803 Lackey, J.S., and Bekker, A. (2018) Rapid emergence of subaerial landmasses and onset of a  
804 modern hydrologic cycle 2.5 billion years ago. *Nature*, 557, 545–548.
- 805 Bleeker, W. (2013) The late Archean record: a puzzle in ca. 35 pieces. *Lithos* 71, 99–134.
- 806 Brown, M. (1998) Unpairing metamorphic belts: *P–T* paths and a tectonic model for the Ryoke Belt,  
807 southwest Japan. *Journal of Metamorphic Geology*, 16, 3–22.
- 808 Brown, M. (2006) Duality of thermal regimes is the distinctive characteristic of plate tectonics since the  
809 Neoproterozoic. *Geology*, 34, 961–964.
- 810 Brown, M. (2007) Metamorphic conditions in orogenic belts: a record of secular change. *International*  
811 *Geology Review*, 49, 193–234.
- 812 Brown, M. (2010) Paired metamorphic belts revisited. *Gondwana Research*, 18, 46–59.
- 813 Brown, M. (2014) The contribution of metamorphic petrology to understanding lithosphere evolution and  
814 geodynamics. *Geoscience Frontiers*, 5, 553–569.
- 815 Brown, M., and Johnson, T. (2018) Invited Centennial Article: Secular change in metamorphism and the  
816 onset of global plate tectonics. *American Mineralogist*, 103, 181–196.
- 817 Brown, M., and Johnson, T. (2019) The 51st Hallimond Lecture—Time’s arrow, time’s cycle: Granulite  
818 metamorphism and geodynamics. *Mineralogical Magazine*, <https://doi.org/10.1180/mgm.2019.19>
- 819 Carlson, W.D., Anderson, S.D., Mosher, S., Davidow, J.S., Crawford, W.D., and Lane, E.D. (2007) High-  
820 pressure metamorphism in the Texas Grenville Orogen: Mesoproterozoic subduction of the  
821 Southern Laurentian continental margin. *International Geology Review*, 49, 99–119.
- 822 Cawood, P.A., Hawkesworth, C.J., Pisarevsky, S.A., Dhuime, B., Capitanio, F.A., and Nebel, O. (2018)  
823 Geological archive of the onset of plate tectonics. *Philosophical Transactions of the Royal*  
824 *Society A*, 376, 20170405.
- 825 Cawood, P.A. and Hawkesworth, C.J. (2019) Earth’s middle age. *Geology*, 42, 503–506.
- 826 Cawood, P.A. and Hawkesworth, C.J. (2019) Continental crustal volume, thickness and area, and their  
827 geodynamic implications. *Gondwana Research*, 66, 116–125.

- 828 Chowdhury, P., Gerya, T., and Chakraborty, S. (2017) Emergence of silicic continents as the lower crust  
829 peels off on a hot plate-tectonic Earth. *Nature Geoscience*, 10, 698–703.
- 830 Clarke, G.L., Powell, R., and Fitzherbert, J.A. (2006) The lawsonite paradox: a comparison of field  
831 evidence and mineral equilibria modelling. *Journal of Metamorphic Geology*, 24, 715–725.
- 832 Condie, K.C. (2018) A planet in transition: The onset of plate tectonics on Earth between 3 and 2 Ga?  
833 *Geoscience Frontiers*, 9, 51–60.
- 834 Condie, K.C., Aster, R.C., and van Hunen, J. (2016) A great thermal divergence in the mantle beginning  
835 2.5 Ga: Geochemical constraints from greenstone basalts and komatiites. *Geoscience Frontiers*, 7,  
836 543–553.
- 837 Condie, K.C., and Kröner, A. (2008) When did plate tectonics begin? Evidence from the geologic record.  
838 *Geological Society of America Special Papers*, 440, 281–294.
- 839 Dhuime, B., Hawkesworth, C.J., Cawood, P.A., and Storey, C.D. (2012) A change in the geodynamics of  
840 continental growth 3 billion years ago. *Science*, 335, 1334–1336.
- 841 Dhuime, B., Hawkesworth, C.J., Delavault, H., Cawood, P.A. (2018) Rates of generation and destruction  
842 of the continental crust: implications for continental growth. *Philosophical Transactions of the*  
843 *Royal Society A*, 376, 20170403.
- 844 Engi, M., Lanari, P., and Kohn, M.J. (2017) Petrochronology: Methods and Applications. *Reviews in*  
845 *Mineralogy and Geochemistry*, 83, 1–577.
- 846 England, P.C., and Richardson, S.W. (1977) The influence of erosion upon the mineral facies of rocks  
847 from different metamorphic environments. *Journal of the Geological Society*, 134, 201–213.
- 848 Erdman, M.E., and Lee, C.-T.A. (2014) Oceanic- and continental-type metamorphic terranes: Occurrence  
849 and exhumation mechanisms. *Earth-Science Reviews*, 139, 33–46.
- 850 Ernst, W.G. (1971) Metamorphic zonations on presumably subducted lithospheric plates from Japan,  
851 California and the Alps. *Contributions to Mineralogy and Petrology*, 34, 43–59.
- 852 Ernst, W.G. (1973) Blueschist metamorphism and P–T regimes in active subduction zones.  
853 *Tectonophysics*, 11, 255–272.

- 854 Flament, N., Coltice, N., and Rey, P.F. (2008) A case for late-Archaean continental emergence from  
855 thermal evolution models and hypsometry. *Earth and Planetary Science Letters*, 275, 326–336.
- 856 Foley, B.J. (2018) The dependence of planetary tectonics on mantle thermal state: applications to early  
857 Earth evolution. *Philosophical Transactions of the Royal Society A*, 376, 20170409.
- 858 Fyfe, W.S., and Turner, F.J. (1966) Reappraisal of the metamorphic facies concept. *Contributions to*  
859 *Mineralogy and Petrology*, 12, 354–364.
- 860 Ganne, J., De Andrade, V., Weinberg, R.F., Vidal, O., Dubacq, B., Kagambega, N., Naba, S., Baratoux,  
861 L., Jessell, M., and Allibon, J. (2012) Modern-style plate subduction preserved in the  
862 Palaeoproterozoic West African craton. *Nature Geoscience*, 5, 60–65.
- 863 Gerya, T. (2014) Precambrian geodynamics: concepts and models. *Gondwana Research*, 25, 442–463.
- 864 Gerya, T.V., Connolly, J.A.D., and Yuen, D.A. (2008) Why is terrestrial subduction one-sided? *Geology*,  
865 36, 43–46.
- 866 Gerya, T.V., Stern, R.J., Baes, M., Sobolev, S.V., and Whattam, S.A. (2015) Plate tectonics on the Earth  
867 triggered by plume-induced subduction initiation. *Nature*, 527, 221–225.
- 868 Glassley, W.E., Korstgard, J.A., Sorensen, K., and Platou, S.W. (2014) A new UHP metamorphic  
869 complex in the ~1.8 Ga Nagssugtoqidian Orogen of West Greenland. *American Mineralogist*, 99,  
870 1315–1334.
- 871 Green, E.C.R., White, R.W., Diener, J.F.A., Powell, R., Holland, T.J.B., and Palin, R.M. (2014) Activity–  
872 composition relations for the calculation of partial melting equilibria in metabasic rocks. *Journal*  
873 *of Metamorphic Geology*, 34, 845–869.
- 874 Gumsley, A.P., Chamberlain, K.R., Bleeker, W., Söderlund, U., de Kock, M.O., Larsson, E.R., and  
875 Bekker, A. (2017) Timing and tempo of the Great Oxidation Event. *Proceedings of the National*  
876 *Academy of Sciences*, 114, 1811–1816.
- 877 Hacker, B.R., Gerya, T.V., and Gilotti, J.A. (2013) Formation and Exhumation of Ultrahigh-Pressure  
878 Terranes. *Elements*, 9, 289–293.

- 879 Hall, R. (2019) The subduction initiation stage of the Wilson cycle. Geological Society, London, Special  
880 Publications, 470, <https://doi.org/10.1144/SP470.3>
- 881 Harrison, T.M., and Wielicki, M.M. (2016) From the Hadean to the Himalaya: 4.4 Ga of felsic terrestrial  
882 magmatism. American Mineralogist, 101, 1348–1359.
- 883 Hawkesworth, C.J., and Brown, M. (2018) Earth dynamics and the development of plate  
884 tectonics. Philosophical Transactions of the Royal Society A, 376, 20180228.
- 885 Herzberg, C. (2019) Origin of high-Mg bimineraleclogite xenoliths in kimberlite: a comment on a  
886 paper by Aulbach and Arndt (2019). Earth and Planetary Science Letters, 510, 231–233.
- 887 Herzberg, C., Condie, K., and Korenaga, J. (2010) Thermal history of the Earth and its petrological  
888 expression. Earth and Planetary Science Letters, 292, 79–88.
- 889 Herzberg, C., Asimow, P.D., Arndt, N., Niu, Y., Leshner, C.M., Fitton, J.G., Cheadle, M.J., and Saunders,  
890 A.D. (2007) Temperatures in ambient mantle and plumes: constraints from basalts, picrites and  
891 komatiites. Geochemistry, Geophysics, Geosystems, 8, Q02006.
- 892 Hess, H.H., 1954. Geological hypotheses and the earth's crust under the oceans. Proceedings of the Royal  
893 Society of London, 222A, 341–348.
- 894 Hoffman, P.F. (2013) The Great Oxidation and a Siderian snowball Earth: MIF-S based correlation of  
895 Paleoproterozoic glacial epochs. Chemical Geology, 362, 143–156.
- 896 Hoffman, P.F., and Schrag, D.P. (2002) The snowball Earth hypothesis: testing the limits of global  
897 change. Terra Nova 14, 129–155.
- 898 Holland, H.D. (2006) The oxygenation of the atmosphere and oceans. Philosophical Transactions of the  
899 Royal Society B, 361, 903–915.
- 900 Holland, T.J.B., Green, E.C.R., and Powell, R. (2018) Melting of peridotites through to granites: a simple  
901 thermodynamic model in the system KNCFMASHTOCr. Journal of Petrology, 59, 881–900.
- 902 Hopkins, M., Harrison, T.M., and Manning, C.E. (2008) Low heat flow inferred from > 4 Gyr zircons  
903 suggests Hadean plate boundary interactions. Nature, 456, 493–496.

- 904 Hyndman, R.D. (2018) Mountain Building Orogeny in Pre-Collision Hot Backarcs: N. Am. Cordillera,  
905 India–Tibet, and Grenville Province. *Journal of Geophysical Research*, doi:  
906 10.1029/2018JB016697
- 907 Isacks, B., Oliver, J., and Sykes, L.R. (1968) Seismology and the New Global Tectonics. *Journal of*  
908 *Geophysical Research*, 73, 5855–5899.
- 909 Johnson, T.E., Brown, M., Kaus, B., and VanTongeren, J.A. (2014) Delamination and recycling of  
910 Archaean crust caused by gravitational instabilities. *Nature Geoscience*, 7, 47–52.
- 911 Johnson, T.E., Brown, M., Goodenough, K.M., Clark, C., Kinny, P.D., and White, R.W. (2016)  
912 Subduction or sagduction? Ambiguity in constraining the origin of ultramafic–mafic bodies in the  
913 Archaean crust of NW Scotland. *Precambrian Research*, 283, 89–105.
- 914 Johnson, T.E., Brown, M., Gardiner, N.J., Kirkland, C.L., and Smithies, R.H. (2017) Earth’s first stable  
915 continents did not form by subduction. *Nature*, 543, 239–243.
- 916 Johnson, T.E., Kirkland, C.L., Gardiner, N.J., Brown, M., Smithies, R.H., and Santosh, M. (2019) Secular  
917 change in TTG compositions: Implications for the evolution of Archaean geodynamics. *Earth and*  
918 *Planetary Science Letters*, 505, 65–75.
- 919 Kaula, W.M., and Phillips, R.J. (1981) Quantitative tests for plate tectonics on Venus. *Geophysical*  
920 *Research Letters*, 8, 1187–1190.
- 921 Korenaga, J. (2013) Initiation and Evolution of Plate Tectonics on Earth: Theories and Observations.  
922 *Annual Review of Earth and Planetary Science*, 41, 117–151.
- 923 Korenaga, J. (2017) Pitfalls in modeling mantle convection with internal heat production. *Journal of*  
924 *Geophysical Research Solid Earth*, 122, 4064–4085.
- 925 Korenaga, J., Planavsky, N.J., and Evans, D.A.D. (2017) Global water cycle and the coevolution of the  
926 Earth's interior and surface environment. *Philosophical Transactions of the Royal Society A*, 375,  
927 20150393.
- 928 Korenaga, J. (2018) Crustal evolution and mantle dynamics through Earth history. *Philosophical*  
929 *Transactions of the Royal Society A*, 376, 20170408.



- 930 Korenaga, J., Planavsky, N.J., and Evans, D.A.D. (2017) Global water cycle and the coevolution of the  
931 Earth's interior and surface environment. *Philosophical Transactions of the Royal Society A*, 375,  
932 20150393.
- 933 Kusky, T.M., Windley, B.F., and Polat, A. (2018) Geological evidence for the operation of plate tectonics  
934 throughout the Archean: Records from Archean paleo-plate boundaries. *Journal of Earth Science*,  
935 29, 1291–1303.
- 936 Kylander-Clark, A.R.C., Hacker, B.R., and Mattinson, C.G. (2012) Size and exhumation rate of ultrahigh-  
937 pressure terranes linked to orogenic stage. *Earth and Planetary Science Letters*, 321, 115–120.
- 938 Lenardic, A. (2018) The diversity of tectonic modes and thoughts about transitions between them.  
939 *Philosophical Transactions of the Royal Society A*, 376, 20170416.
- 940 Lenardic, A., Moresi, L., Jellinek, A.M., O'Neill, C.J., Cooper, C.M., and Lee, C.T. (2011) Continents,  
941 supercontinents, mantle thermal mixing, and mantle thermal isolation: Theory, numerical  
942 simulations, and laboratory experiments. *Geochemistry, Geophysics, Geosystems*, 12, Q10016.
- 943 Le Pichon, X. (1968) Sea floor spreading and continental drift. *Journal of Geophysical Research*, 73,  
944 3661–3697.
- 945 Li, Z.X., Mitchell, R.N., Spencer, C.J., Ernst, R., Pisarevsky, S., Kirscher, U., and Murphy, J.B. (2019)  
946 Decoding Earth's rhythms: Modulation of supercontinent cycles by longer superocean episodes.  
947 *Precambrian Research*, 323, 1–5.
- 948 McKenzie, D.P., and Parker, R.L. (1967) North Pacific – An example of tectonics on a sphere. *Nature*,  
949 216, 1276–1280.
- 950 Magni, V., Bouilhol, P., and van Hunen, J. (2014) Deep water recycling through time. *Geochemistry*,  
951 *Geophysics, Geosystems*, 15, 4203–4216.
- 952 Malusà, M. G., C. Faccenna, C., Baldwin, S.L., Fitzgerald, P.G., Rossetti, F., Balestrieri, M.L., Danisík,  
953 M., Ellero, A., Ottria, G., and C. Piromallo, C. (2015), Contrasting styles of (U)HP rock

- 954 exhumation along the Cenozoic Adria–Europe plate boundary (Western Alps, Calabria, Corsica).  
955 *Geochemistry Geophysics Geosystems*, 16, 1786–1824.
- 956 Maunder, B., van Hunen, J., Bouilhol, P., and Magni, V. (2014) Modeling Slab Temperature: A  
957 Reevaluation of the Thermal Parameter. *Geochemistry, Geophysics, Geosystems*, 20, 673–687.
- 958 Meert, J.G., and Santosh, M. (2017) The Columbia supercontinent revisited. *Gondwana Research*, 50, 67–  
959 83.
- 960 Miyashiro, A. (1961) Evolution of metamorphic belts. *Journal of Petrology*, 2, 277–311.
- 961 Miyashiro, A. (1972) Metamorphism and related magmatism in plate tectonics. *American Journal of*  
962 *Science*, 272, 629–656.
- 963 Miyashiro, A. (1973) Paired and unpaired metamorphic belts. *Tectonophysics*, 17, 241–254.
- 964 Morgan, W.J. (1968) Rises, Trenches, Great Faults, and Crustal Blocks. *Journal of Geophysical Research*,  
965 73, 1959–1982.
- 966 Moyen, J.-F., and van Hunen, J. (2012) Short-term episodicity of Archaean plate tectonics. *Geology*, 40,  
967 451–454.
- 968 Nicoli, G., and Dyck, B. (2018) Exploring the metamorphic consequences of secular change in the  
969 siliciclastic compositions of continental margins. *Geoscience Frontiers*, 9, 967–975.
- 970 O'Neill, C., Lenardic, A., Moresi, L., Torsvik, T.H., and Lee, C.-T.A. (2007) Episodic Precambrian  
971 subduction. *Earth and Planetary Science Letters*, 262, 552–562.
- 972 O'Neill, C., Marchi, S., Zhang, S., and Bottke, W. (2017) Impact-driven subduction on the Hadean Earth.  
973 *Nature Geoscience*, 10, 793–797.
- 974 O'Neill, C., Turner, S. and Rushmer, T. (2018) The inception of plate tectonics: a record of failure. *re.*  
975 *Philosophical Transactions of the Royal Society A*, 376, 20170414.
- 976 Oreskes, N. (2002) *Plate tectonics: An insider's history of the modern theory of the Earth*. Westview  
977 Press, Boulder, CO, USA, 448 pages.
- 978 Oxburgh, E.R., and Turcotte, D.L. (1971) Origin of paired metamorphic belts and crustal dilation in  
979 island arc regions. *Journal of Geophysical Research*, 76, 1315–1327.

- 980 Palin, R.M., and Dyck, B. (2018) Metamorphic consequences of secular changes in oceanic crust  
981 composition and implications for uniformitarianism in the geological record. *Geoscience*  
982 *Frontiers*, 9, 1009–1019.
- 983 Palin, R.M., and White, R.W. (2016) Emergence of blueschists on Earth linked to secular changes in  
984 oceanic crust composition. *Nature Geoscience*, 9, 60–64.
- 985 Pearce, J.A. (2008) Geochemical fingerprinting of oceanic basalts with applications to ophiolite  
986 classification and the search for Archean oceanic crust. *Lithos*, 100, 14–48.
- 987 Pearce, J.A. (2014) Geochemical Fingerprinting of the Earth’s Oldest Rocks. *Geology*, 42, 175–176.
- 988 Pehrsson, S.J., Berman, R.G., Eglington, B., and Rainbird, R. (2013) Two Neoproterozoic supercontinents  
989 revisited: The case for a Rae family of cratons. *Precambrian Research*, 232, 27–43.
- 990 Penniston-Dorland, S.-C., Kohn, M.J., and Manning, C.E. (2015) The global range of subduction zone  
991 thermal structures from exhumed blueschists and eclogites: Rocks are hotter than models. *Earth*  
992 *and Planetary Science Letters*, 428, 243–254.
- 993 Perchuk, A.L., Safonov, O.G., Smit, C.A., van Reenen, D.D., Zakharov, V.S., Gerya, T.V., 2018.  
994 Precambrian ultra-hot orogenic factory: making and reworking of continental crust.  
995 *Tectonophysics*, 746, 572–586
- 996 Piccardo, G.B., Rampone, E., and Romairone, A. (2002) Formation and composition of the oceanic  
997 lithosphere of the Ligurian Tethys: Inferences from the Ligurian ophiolites. *Ofioliti*, 27, 145–161.
- 998 Powell, R., and Holland, T.J.B. (2008). On thermobarometry. *Journal of Metamorphic Geology*, 26, 155–  
999 179.
- 1000 Putirka, K. (2016) Rates and styles of planetary cooling on Earth, Moon, Mars, and Vesta, using new  
1001 models for oxygen fugacity, ferric-ferrous ratios, olivine-liquid Fe-Mg exchange, and mantle  
1002 potential temperature. *American Mineralogist*, 101, 819–840.
- 1003 Rey, P.F., and Coltice, N. (2008) Neoproterozoic lithospheric strengthening and the coupling of Earth's  
1004 geochemical reservoirs. *Geology*, 36, 635–638.

- 1005 Rey, P. F., Coltice, N., and Flament, N. (2014) Spreading continents kick-started plate tectonics. *Nature*,  
1006 513, 405–408.
- 1007 Rozel, A.B., Golabek, G.J., Jain, C., Tackley, P.J., and Gerya, T. (2017) Continental crust formation on  
1008 early Earth controlled by intrusive magmatism. *Nature*, 545, 332–335.
- 1009 Scholl, D.W., and von Huene, R. (2010) Subduction zone recycling processes and the rock record of  
1010 crustal suture zones. *Canadian Journal of Earth Sciences*, 47, 633–654.
- 1011 Sizova, E., Gerya, T., Brown, M., and Perchuk, L.L. (2010) Subduction styles in the Precambrian: insight  
1012 from numerical experiments. *Lithos*, 116, 209–229.
- 1013 Sizova, E., Gerya, T., and Brown, M. (2012) Exhumation mechanisms of melt-bearing ultrahigh pressure  
1014 crustal rocks during collision of spontaneously moving plates. *Journal of Metamorphic Geology*,  
1015 30, 927–955.
- 1016 Sizova, E., Gerya, T., and Brown, M. (2014) Contrasting styles of Phanerozoic and Precambrian  
1017 continental collision. *Gondwana Research*, 25, 522–545.
- 1018 Sizova, E., Gerya, T., Stüwe, K., and Brown, M. (2015) Generation of felsic crust in the Archean: A  
1019 geodynamic modeling perspective. *Precambrian Research*, 27, 198–224.
- 1020 Smithies, R.H., Ivanic, T.J., Lowrey, J.R., Morris, P.A., Barnes, S.J., Wyche, S., and Lu, Y.-J. (2018)  
1021 Two distinct origins for Archean greenstone belts. *Earth and Planetary Science Letters*, 487, 106–  
1022 116.
- 1023 Smrekar, S.E., Davaille, A., and Sotin, C. (2018) Venus interior structure and dynamics. *Space Science*  
1024 *Reviews*, 214, UNSP 88.
- 1025 Sobolev, S.V., and Brown, M. (2019) Major surface erosion events were a key control on the emergence  
1026 and evolution of plate tectonics on Earth. *Nature*, revised.
- 1027 Spencer, C.J., Cawood, P.A., Hawkesworth, C.J., Raub, T.D., Prave, A.R., and Roberts, N.M.W. (2014)  
1028 Proterozoic onset of crustal reworking and collisional tectonics: Reappraisal of the zircon oxygen  
1029 isotope record. *Geology*, 42, 451–454.

- 1030 Spencer, C.J., Murphy, J.B., Kirkland, C.L., Liu, Y.B., and Mitchell, R.N. (2018) A Palaeoproterozoic  
1031 tectono-magmatic lull as a potential trigger for the supercontinent cycle. *Nature Geoscience*, 11,  
1032 97–101.
- 1033 St-Onge, M.R., Searle, M.P., and Wodicka, N. (2006) Trans-Hudson orogen of North America and  
1034 Himalaya-Karakoram-Tibetan orogen of Asia: structural and thermal characteristics of the lower  
1035 and upper plates. *Tectonics* 25, 1–22.
- 1036 St-Onge, M.R., Van Gool, J.A.M., Garde, A.A. & Scott, D.J. (2009) Correlation of Archaean and  
1037 Palaeoproterozoic units between northeastern Canada and western Greenland: constraining the  
1038 pre-collisional upper plate accretionary history of the Trans-Hudson orogen. Geological Society,  
1039 London, Special Publication, 318, 193–235.
- 1040 Stern, R. J. (2005) Evidence from ophiolites, blueschists, and ultrahigh-pressure metamorphic terranes  
1041 that the modern episode of subduction tectonics began in Neoproterozoic time. *Geology*, 33, 557–  
1042 560.
- 1043 Stern, R.J. (2018) The evolution of plate tectonics. *Philos. Trans. R. Soc. A Math. Phys. Eng. Sci.* 376,  
1044 20170406.
- 1045 Stern, R.J., and Scholl, D.W. (2010) Yin and yang of continental crust creation and destruction by plate  
1046 tectonic processes. *International Geology Review*, 52, 1–31.
- 1047 Sykes, L.R. (1967) Mechanism of earthquakes and nature of faulting on the mid-ocean ridges. *Journal of*  
1048 *Geophysical Research*, 72, 2131–2153.
- 1049 Tang, M., Chen, K., and Rudnick, R.L. (2016) Archean upper crust transition from mafic to felsic marks  
1050 the onset of plate tectonics. *Science*, 351, 372–375.
- 1051 Turner, F.J. (1968) *Metamorphic petrology. Mineralogical and field aspects.* McGrawh-Hill, 403 pp.
- 1052 Turner, S., Rushmer, T., Reagan, M., and Moyen, J.-F. (2014) Heading down early on? Start of  
1053 subduction on Earth. *Geology*, 42, 139–142.

- 1054 Tsujimori, T., Sisson, V.B., Liou, J.G., Harlow, G.E., and Sorensen, S.S. (2006) Very-low-temperature  
1055 record of the subduction process: A review of worldwide lawsonite eclogites. *Lithos*, 92, 609–  
1056 624.
- 1057 Van Hunen, J., and Moyen, J.-F. (2012) Archean Subduction: Fact or Fiction? *Annual Review of Earth  
1058 and Planetary Science*, 40, 195–219.
- 1059 van Hunen, J., and van den Berg, A.P. (2008) Plate tectonics on the early Earth: Limitations imposed by  
1060 strength and buoyancy of subducted lithosphere. *Lithos*, 103, 217–235.
- 1061 van Keken, P.E., Hacker, B.R., Syracuse, E.M., and Abers, G.A. (2011) Subduction factory 4: Depth-  
1062 dependent flux of H<sub>2</sub>O from subducting slabs worldwide. *Journal of Geophysical Research*, 116,  
1063 B01401.
- 1064 Van Keken, P.E., Wada, I., Abers, G.A., Hacker, B.R., and Wang, K. (2018) Mafic high-pressure rocks  
1065 are preferentially exhumed from warm subduction settings. *Geochemistry, Geophysics,  
1066 Geosystems*, 19, 2934–2961.
- 1067 Vine, F.J., and Matthews, D.H. (1963) Magnetic anomalies over oceanic ridges. *Nature*, 199, 947–949.
- 1068 Wada, I., and Wang, K. (2009) Common depth of slab–mantle decoupling: reconciling diversity and  
1069 uniformity of subduction zones. *Geochemistry, Geophysics, Geosystems*, 10, Q10009.
- 1070 Warren, C.J. (2013) Exhumation of (ultra-)high-pressure terranes: concepts and mechanisms. *Solid Earth*,  
1071 4, 75–92.
- 1072 Wei, C.J., and Clarke, G.L. (2011) Calculated phase equilibria for MORB compositions: a reappraisal of  
1073 the metamorphic evolution of lawsonite eclogite. *Journal of Metamorphic Geology*, 29, 939–952.
- 1074 Weller, O.M., and St-Onge, M.R. (2017) Record of modern-style plate tectonics in the Palaeoproterozoic  
1075 Trans-Hudson orogen. *Nature Geoscience*, 10, 305–311.
- 1076 Weller, O.M., Wallis, S.R., Aoya, M., and Nagaya, T. (2015) Phase equilibria modelling of blueschist and  
1077 eclogite from the Sanbagawa metamorphic belt of southwest Japan reveals along-strike  
1078 consistency in tectonothermal architecture. *Journal of Metamorphic Geology*, 33, 579–596.

- 1079 White, R.W., Powell, R., Holland, T.J.B., Johnson, T.E., and Green, E.C.R. (2014) New mineral activity–  
1080 composition relations for thermodynamic calculations in metapelitic systems. *Journal of*  
1081 *Metamorphic Geology*, 32, 261–286.
- 1082 Wilson, J.T. (1965) A new class of faults and their bearing on continental drift. *Nature*, 207, 343–347.
- 1083 Xia, B., Zhang, L., Du, Z., and Xu, B. (2019) Petrology and age of Precambrian Aksu blueschist, NW  
1084 China. *Precambrian Research*, <https://doi.org/10.1016/j.precamres.2017.12.041>
- 1085 Xia, B., Brown, M., Wang, L., Wang, S.-J., and Piccoli, P., 2018. Phase equilibria modeling of MT–UHP  
1086 eclogite: a case study of coesite eclogite at Yangkou, Sulu belt, Eastern China. *Journal of*  
1087 *Petrology*, 59, 1253–1280.
- 1088 Xu, C., Kynický, J., Song, W., Tao, R., Lü, Z., Li, Y., Yang, Y., Pohanka, M., Galiova, M.V., Zhang, L.,  
1089 and Fei, Y. (2018) Cold deep subduction recorded by remnants of a Paleoproterozoic carbonated  
1090 slab. *Nature Communications*, 9, 1–8.
- 1091
- 1092 Young, G.M., von Brunn, V., Gold, D.J.C., and Minter, W.E.L. (1998) Earth's oldest reported  
1093 glaciation: Physical and chemical evidence from the Archean Mozaan Group (similar to  
1094 2.9 Ga) of South Africa. *Journal of Geology*, 106, 523–538.
- 1095 Yong, W.J., Zhang, L., Hall, C.M., Mukasa, S.B., and Essene, E.J. (2013) The Ar-40/Ar-39 and  
1096 Rb-Sr chronology of the Precambrian Aksu blueschists in western China. *Journal of*  
1097 *Asian Earth Sciences*, 63, 197–205.
- 1098 Zack, T., Rivers, T., Brumm, R., and Kronz, A. (2004) Cold subduction of oceanic crust: implications  
1099 from a lawsonite eclogite from the Dominican Republic. *European Journal of Mineralogy*, 16,  
1100 909–916.
- 1101
- 1102 MANUSCRIPT RECEIVED
- 1103 MANUSCRIPT ACCEPTED

1104 MANUSCRIPT HANDLED BY

1105

1106 **Endnote:**

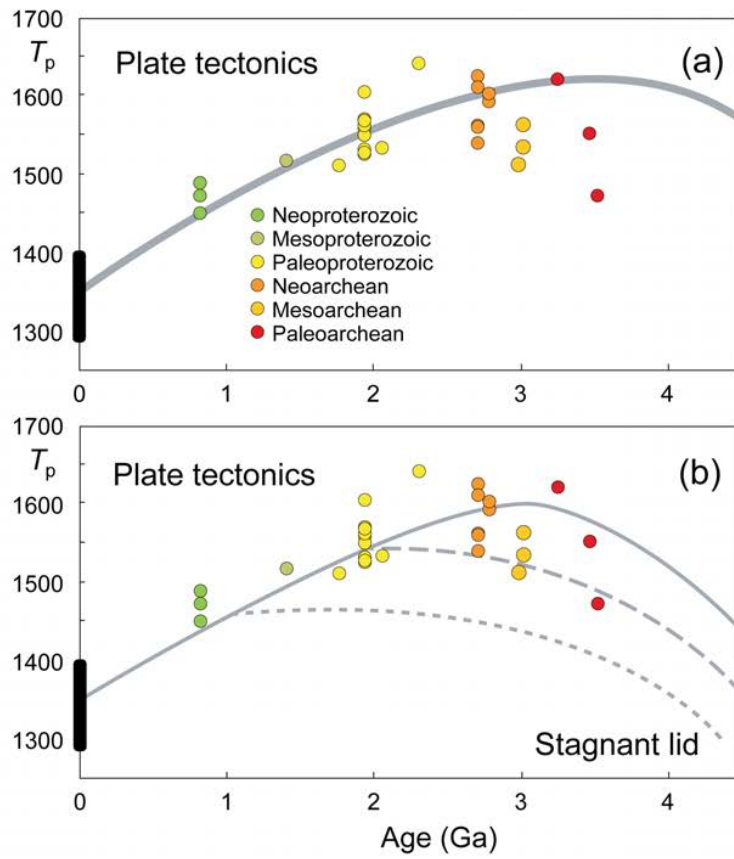
1107 <sup>1</sup>Deposit item AM-19-?????, Supplemental Material. Deposit items are free to all readers and found on the MSA

1108 web site, via the specific issue's Table of Contents (go to <http://www.minsocam.org/MSA/AmMin/TOC/2019/...>

1109 data.html).

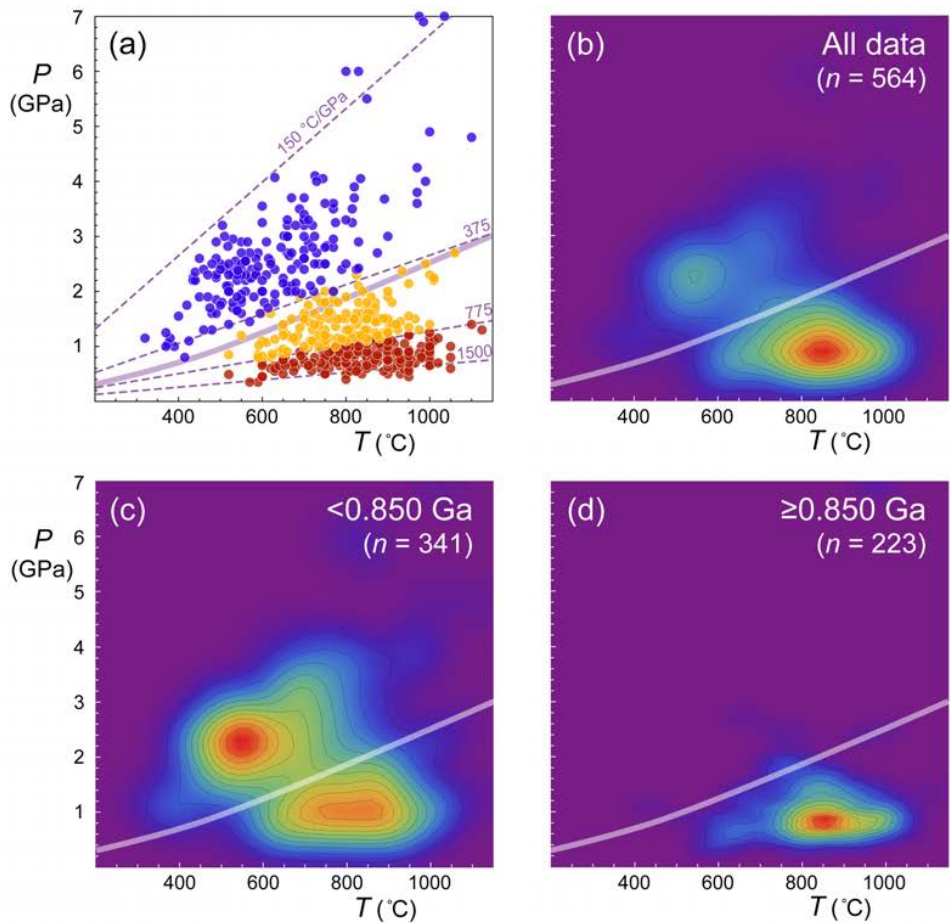
1110





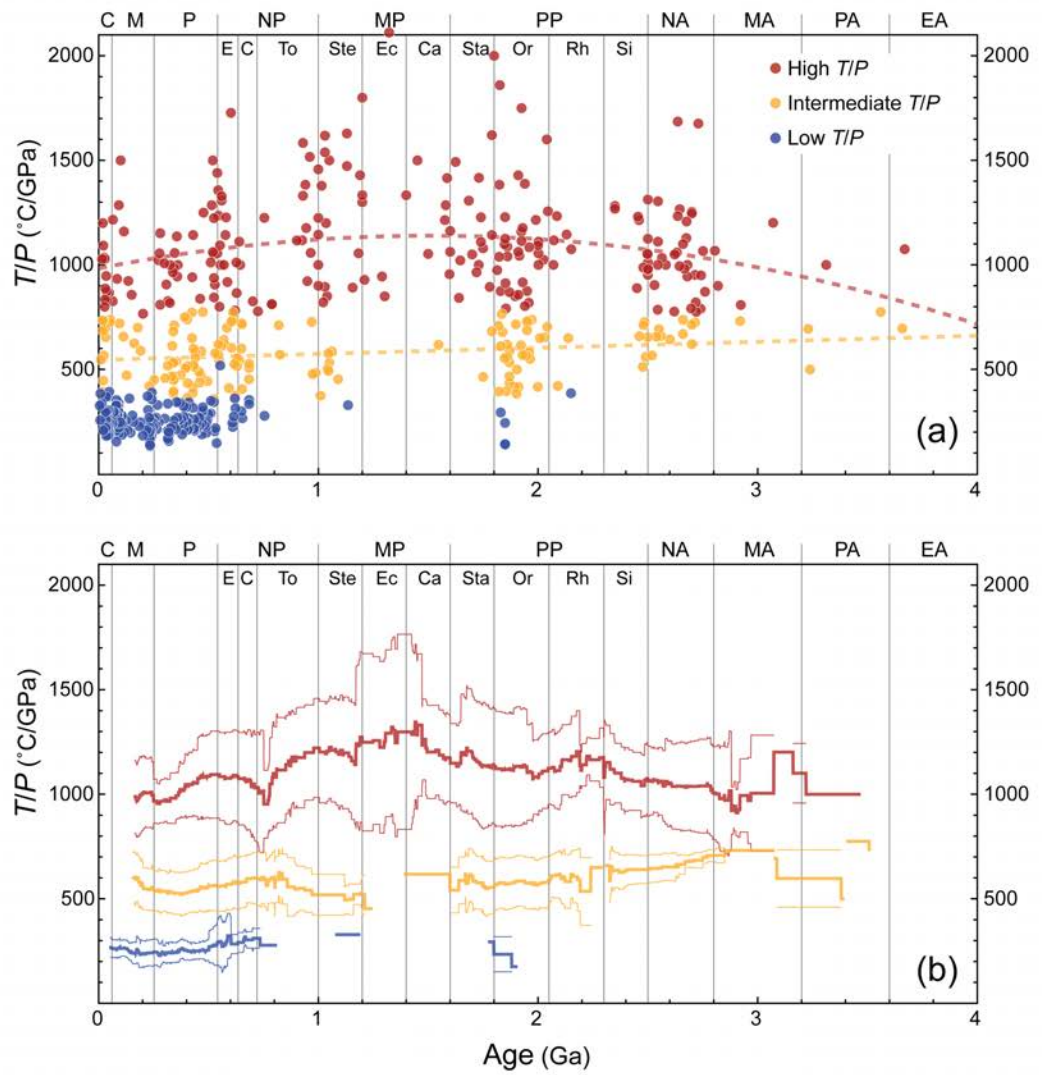
Brown & Johnson – Figure 1

1112 **FIGURE 1.** The evolution of mantle potential temperature ( $T_p$ ) modelled with (a) constant surface  
1113 heat flow and low present-day Urey ratio of 0.22 (after Korenaga, 2017) and (b) with a switch in  
1114 heat-flow scaling and relatively low present-day Urey ratio of 0.35 from stagnant lid (lower heat  
1115 flow) to plate tectonics (higher heat flow) at 3 Ga, 2 Ga or 1 Ga (after Korenaga, 2013). The TP  
1116 data are taken from Herzberg et al. (2010), using the modified ages of Johnson et al. (2014).  
1117



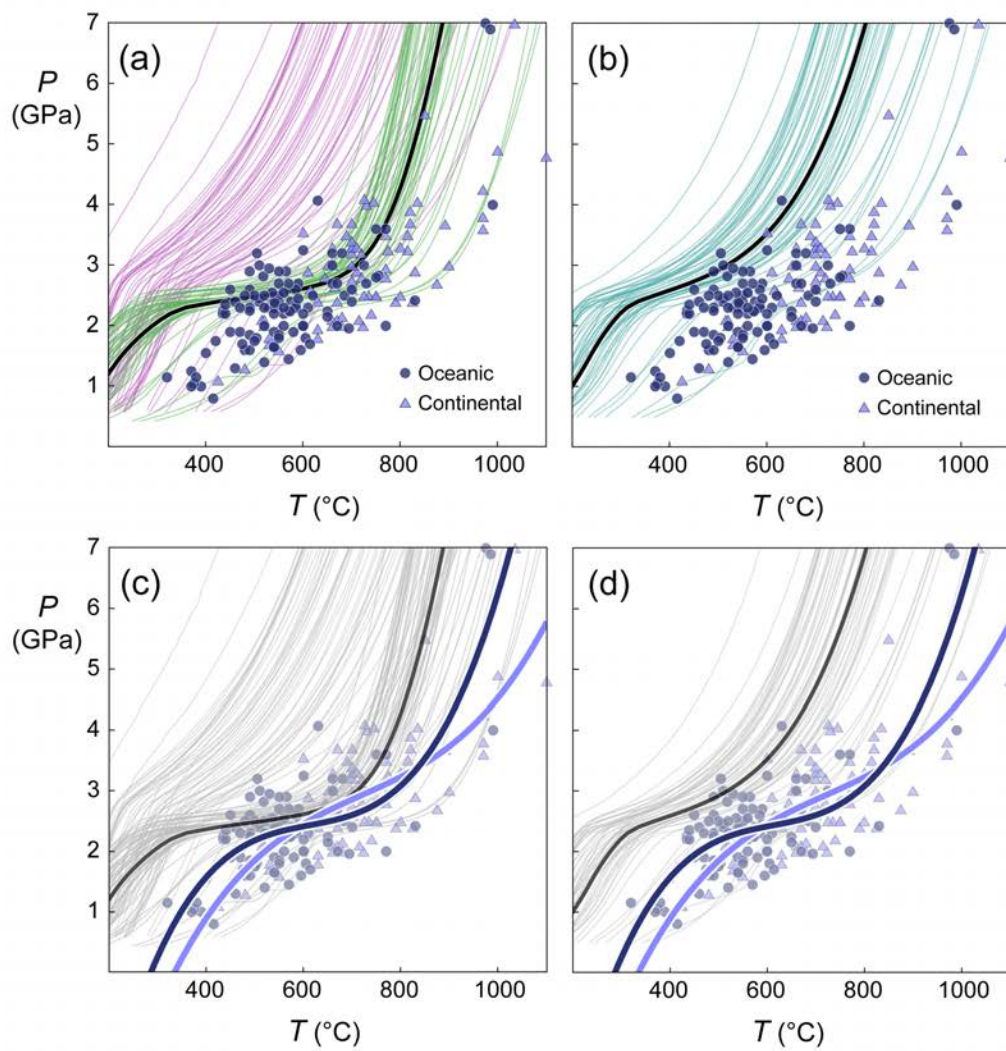
Brown & Johnson – Figure 2

1119 **FIGURE 2.** Conditions of ‘peak’ metamorphism for 564 localities with robust pressure ( $P$ ),  
1120 temperature ( $T$ ) and age ( $t$ ) grouped by type (a), with the ‘normal’ geotherm from Stüwe (2007;  
1121 thick dashed line) and representative thermal gradients (thin dashed lines). (a) Three types of  
1122 metamorphism are distinguished based on thermobaric ratios ( $T/P$ ), as follows: low T/P  
1123 metamorphism in blue ( $n = 189$ ), intermediate T/P metamorphism in orange ( $n = 152$ ), and high  
1124 T/P metamorphism in red ( $n = 223$ ). (b) Shows a plot of all data contoured for density, (c) shows  
1125 a plot of data  $<850$  Ma in age contoured for density, and (d) shows a plot of data  $\geq 850$  Ma in age  
1126 contoured for density. Note, the ‘normal’ geotherm only applies to the tectonic regime since 850  
1127 Ma; before that time the average crustal geotherm must have been hotter since all the data plot  
1128 below the ‘normal’ geotherm. In this and subsequent figures, data were contoured for density  
1129 using DensityPlot in Wolfram Mathematica.  
1130



Brown & Johnson – Figure 3

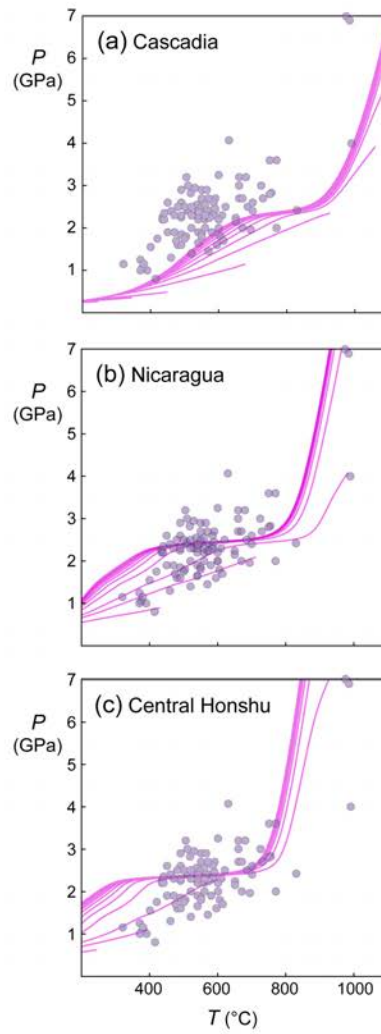
1132 **FIGURE 3.** (a) Metamorphic thermobaric ratios ( $T/P$ ) for 564 localities grouped by type plotted  
1133 against age. The three types of metamorphism are high  $T/P$  in red, intermediate  $T/P$  in orange  
1134 and low  $T/P$  in blue. The dashed lines show a second-order polynomial regression of the data for  
1135 the high  $T/P$  (red) and a linear regression of the data for the intermediate  $T/P$  (orange) types,  
1136 respectively. (b) Moving means (with one sigma uncertainty) of the thermobaric ratios ( $T/P$ ) for  
1137 high and intermediate  $T/P$  metamorphism calculated every 1 Myr within a moving 300 Myr  
1138 window, and for low  $T/P$  metamorphism calculated every 1 Myr within a moving 100 Myr  
1139 window.  
1140



Brown & Johnson – Figure 4

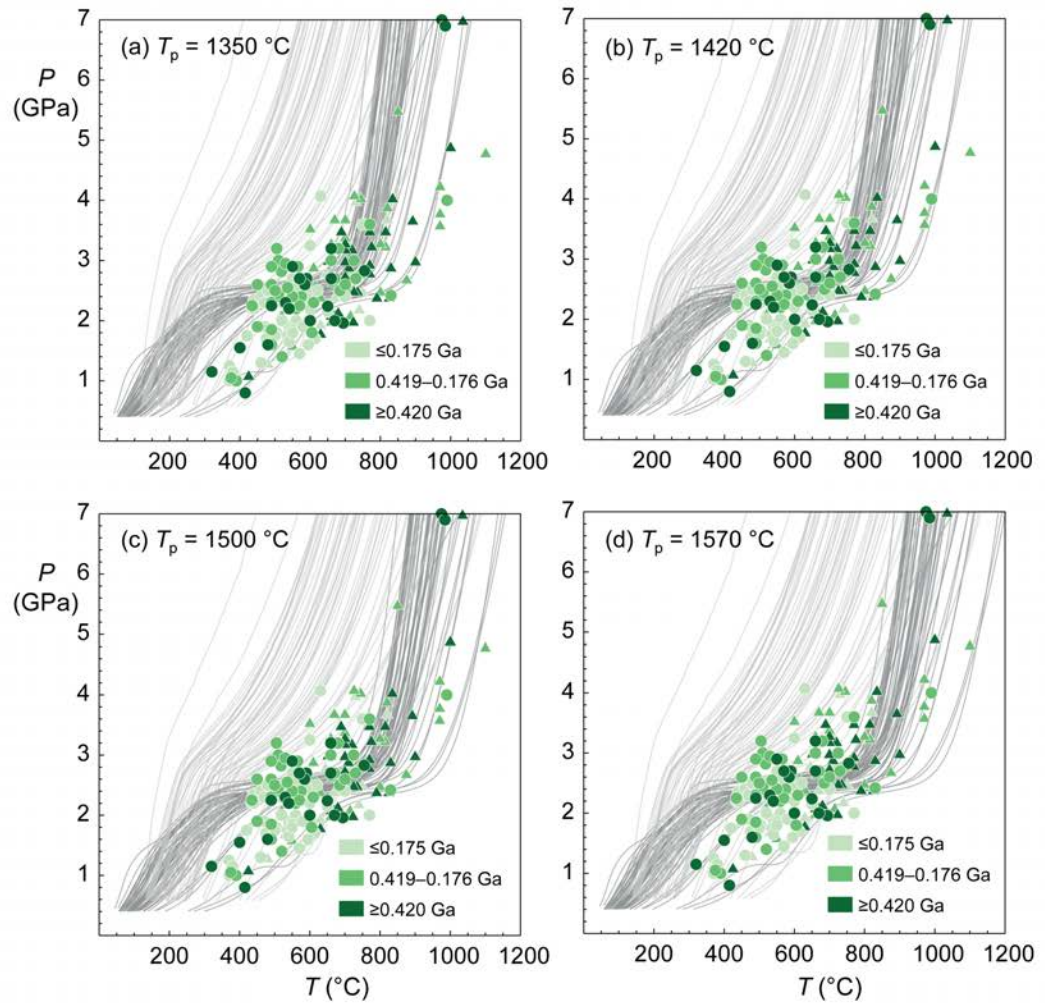
1142 **FIGURE 4.** Comparison between thermal models of Van Keken et al. (2011, as discussed in Van  
1143 Keken et al., 2018; models without shear heating,  $n = 56$ ) and peak  $P$ - $T$  conditions of oceanic  
1144 low T/P metamorphic rocks ( $n = 105$ ). (a) Green lines are slab  $P$ - $T$  paths for the uppermost  
1145 oceanic crust (OC; 0.5 km below top of slab (black line is average of 56 models)) and magenta  
1146 lines are lowermost OC (6.5 km into the OC). (b)  $P$ - $T$  conditions averaged over the OC in each  
1147 model (teal lines; black line is average of 56 models), i.e. this assumes the possibility of  
1148 exhumation from any level in the oceanic crust. In (c) and (d), we show the same information as  
1149 (a) and (b), but in greyscale, together with the third degree polynomial regression through each  
1150 of the oceanic and continental data. Interpretation of this figure is discussed in more detail in the  
1151 text.  
1152





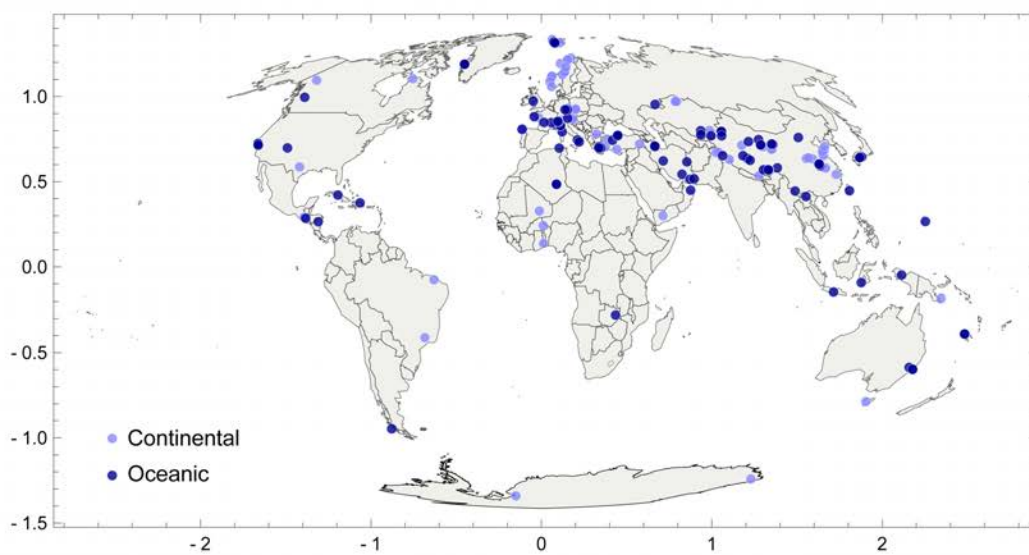
Brown & Johnson – Figure 5

1154 **FIGURE 5.** Peak metamorphic conditions of oceanic low T/P metamorphic rocks vs the thermal  
1155 evolution of the top of the ocean crust for: a. the warm Cascadia, b. the intermediate Nicaragua,  
1156 and c. the cold Central Honshu models of Van Keken et al. (2018; models without shear  
1157 heating). From low  $P$ , the first two lines are for 1 and 2 Ma after subduction initiation, and  
1158 thereafter the lines are for 3 to 30 Ma at 3 Ma intervals; each  $P$ - $T$  path is limited to the  $P$  at the  
1159 tip of the slab at each time instant.  
1160



Brown & Johnson – Figure 6

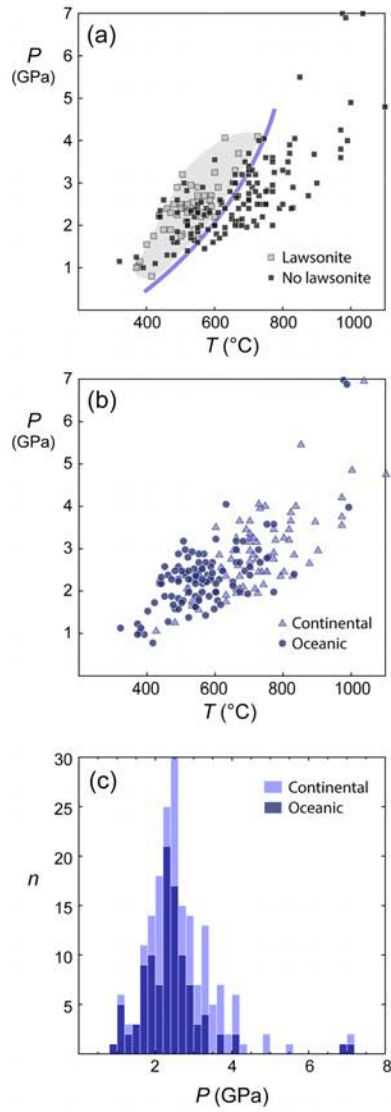
1162 **FIGURE 6.** Comparison between thermal models of van Keken et al. (2011, as discussed in van  
1163 Keken et al., 2018; models without shear heating,  $n = 56$ ) for different mantle  $T_P$  of 1350 °C (a),  
1164 1420 °C (b), 1500 °C (c) and 1570 °C (d), and peak  $P-T$  conditions of low T/P metamorphic  
1165 rocks (these thermal models at elevated  $T_P$  are unpublished and were provided by P. Van Keken  
1166 as a personal communication, January 2019). Darker grey lines are slab  $P-T$  paths for the  
1167 uppermost oceanic crust (OC; 0.5 km below top of slab) and light grey lines are lowermost OC  
1168 (6.5 km into the OC). The data are separated into oceanic (filled circles;  $n = 105$ ) and continental  
1169 (filled triangles  $n = 84$ ), and by age as follows: dark green = 420 Ma and older; mid green = 419–  
1170 176 Ma; and, light green = 175 Ma and younger. Interpretation of this figure is discussed in more  
1171 detail in the text.  
1172



Brown & Johnson – Figure 7

1174 **FIGURE 7.** Map to show the present-day geographic distribution of low T/P metamorphic rocks.

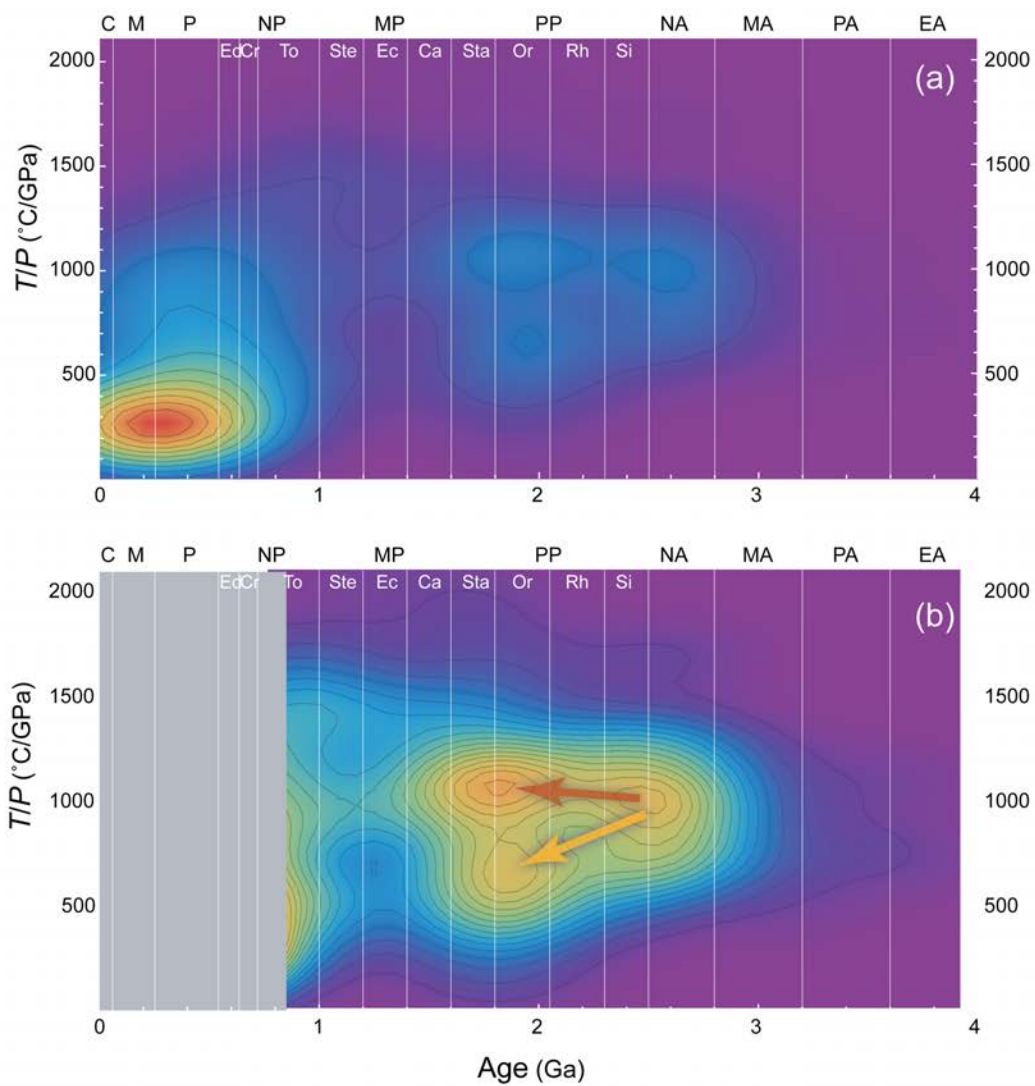
1175



Brown & Johnson – Figure 8

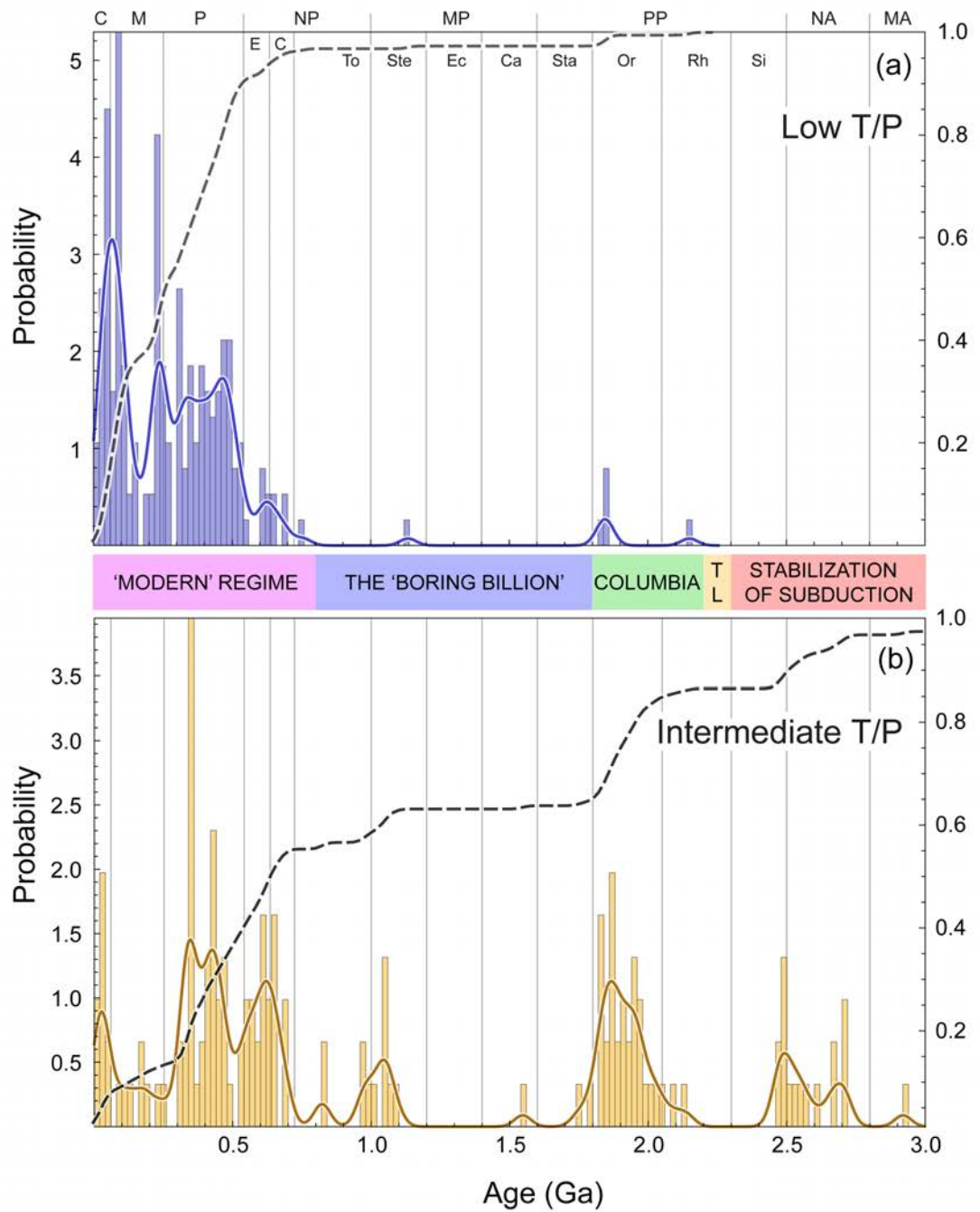
1177 **FIGURE 8.** a.  $P$ – $T$  for rocks with Lws (or pseudomorphs) vs without Lws (line represents the  
1178 approximate position of the Lws-out reaction). b.  $P$ – $T$  conditions for low T/P type  
1179 metamorphism separated into oceanic (dark blue symbols) and continental (light blue symbols)  
1180 varieties. c. Histogram of peak metamorphic pressures for low T/P type metamorphism separated  
1181 into oceanic (dark blue symbols) and continental (light blue symbols) varieties.  
1182





Brown & Johnson – Figure 9

1184 **FIGURE 9.** a. Metamorphic  $T/P$  data from Figure 3 contoured for density. b. Metamorphic  $T/P$   
1185 data for localities >850 Ma in age contoured for density to emphasise the development of  
1186 bimodality from the Archean through the Proterozoic (in (a), this pattern is swamped by the low  
1187  $T/P$  data that are <850 Ma in age).  
1188



Brown & Johnson – Figure 10

1190 **FIGURE 10.** (a) Histogram of ages, probability density function and cumulative smooth kernel  
1191 density estimate for low T/P type metamorphism. (b) Histogram of ages, probability density  
1192 function and cumulative smooth kernel density estimate for intermediate T/P type  
1193 metamorphism. In the tectonic summary bar, TL is tectonomagmatic lull.